DEPT. DE QUÍMICA ANALÍTICA
i QUÍMICA ORGÀNICA
Universitat Rovira i Virgili

Stereoselective synthesis of cyclopropenone-based ceramide derivatives as potential dihydroceramide desaturase 1 inhibitors

Master's degree in Synthesis, Catalysis and Molecular Design

Adrià Figueras Boldó

2021-22

Supervised by Prof. M. Isabel Matheu Malpartida

Acknowledgements

Voldria començar donant gràcies a la tutora, Maribel Matheu, per totes les explicacions, correccions i suggeriments que ha aportat al llarg de tot aquest treball.

També voldria agrair als companys del grup SINTCARB: Albert, Javier, Èric, Jordi, Miguel, Isabel, Andrea, Haidi, Anna, Paula i Jorge, per tots els moments viscuts, així com una menció especial al Pablo, el company de vitrina que ha aconseguit que m'agradi Supertramp i autor dels consells que tant m'han ajudat en la realització d'aquest treball de fi de màster que ara tens a les mans.

Finalment, penso que aquests agraïments no estarien complets sense un record a tots els amics que m'han acompanyat al llarg d'aquesta aventura i n'han fet una experiència inoblidable, moltes gràcies a tots!

Table of contents

Abbreviations and acronyms

AcOH: acetic acid

anh.: anhydrous

ap: apparent

Boc: *tert*-butyloxycarbonyl

br: broad

BuLi: butyl lithium

COSY: correlation spectroscopy

d: doublet

DCM: dichloromethane

dd: doublet of doublets

Des1: dihydroceramide desaturase 1

DMF: dimethylformamide

dt: doublet of triplets

EDC: *N*-(3-Dimethylaminopropyl)-*N*'-ethyl carbodiimide

ESI: electrospray ionization

Et_2O: diethyl ether

ETHE1: ethylmalonic encephalopathy 1

EtOAc: ethyl acetate

GDT: global distance test

Glu: glutamate

h: hours

HMBC: heteronuclear multiple bond correlation

HMPA: hexamethylphosphorotriamide

HOBt: hydroxybenzotriazole

HRMS: high resolution mass spectrometry

HSQC: heteronuclear single quantum coherence spectroscopy

IC_{50}: half maximal inhibitory concentration

IR: Infrared

J: coupling constant

Ki: inhibitory constant

m: multiplet

MeOH: methanol

min: minutes

NPg: *N*-protected group

Nu: nucleophile

p: quintuplet

q: quadruplet

r.t.: room temperature

R_f: retention factor

s: singlet

sat.: saturated

sol.: solution

t: triplet

td: triplet of doublets

TFA: trifluoroacetic acid

THF: tetrahydrofuran

TMS: trimethylsilyl

Tyr: tyrosine

Abstract

The view on dihydroceramide, generally regarded to be innocuous, changed after the revelation that it might have regulatory roles in biology. In this scenario, dihydroceramide desaturase 1 (Des1) stands out as a new therapeutic target since it catalyses the formation of a double bond in dihydroceramide to convert it to ceramide in the *de novo* synthesis of this sphingolipid. Inhibition of Des1 would cause an accumulation of dihydroceramide, which has been related to cell growth arrest and apoptosis. However, the limited number of Des1 inhibitors described until now and the lack of a crystalline structure of the enzyme hamper the understanding of its inhibition mechanism. For this reason, the synthesis of new inhibitors is necessary to shed light on this field.

In this master's thesis degree, the stereoselective synthesis of cyclopropenone-based ceramide derivatives as potential Des 1 inhibitors will be presented. By harnessing the singular reactivity of cyclopropenones one of the potential Des1 inhibitors, bearing a 1,2-dichalcogen heterocycle, has been synthesized in an effective and time-saving manner *via* late-stage functionalization.

All targeted molecules have been rationalized for the aforementioned purpose, present all known requirements for Des1 inhibitory activity and docking studies, made in collaboration with Dr. Xavier Barril from University of Barcelona (UB), support their potential as Des1 inhibitors. The synthetic pathway features the obtaining of a protected cyclopropenone moiety and its stereoselective addition to (*S*)-Garner's aldehyde, a compound from the chiral pool. This key step, followed by a concomitant deprotection and further *N*-acylation will allow to obtain the first targeted compound in a 6-step synthesis in an overall yield of 24%. A late-stage functionalization will allow obtaining the second targeted compound in an overall 7-step synthesis in 12% yield.

Both synthetized compounds will be evaluated soon as Des1 inhibitors at Dra. Gemma Fabriàs laboratory (Institut de Química Avançada de Catalunya, IQAC-CSIC, Barcelona).

1. Introduction

1.1. Relationship between sphingolipids and cancer

Sphingolipids were discovered in 1874 by Johann Ludwig Thudichum when fractionating brain extracts with ethanol. The root of the word sphingo, "sphinx", comes from the Greek mythology being half woman half winged lion who posed riddles that had to be solved. This description correlates to the at the time unusual structure of these compounds, which have a polar head attached to an apolar fragment.[1]

Nowadays, the biological function of these compounds has been extensively studied and there is sufficient scientific evidence to affirm that the presence of certain sphingolipids has decisive effects on the regulation of cell survival, differentiation, and death (from now on, apoptosis).[2]

Sphingolipids consist of a wide range of compounds formed from the modification of a common skeleton consisting of a long aliphatic chain with a length of 15 carbon atoms in the case of mammals, a polar head that contains a primary hydroxyl group and a 2,3-aminoalcohol moiety with (2*S*, 3*R*) configuration. When the amino group is attached to a fatty acid, a ceramide is formed (Figure 1).

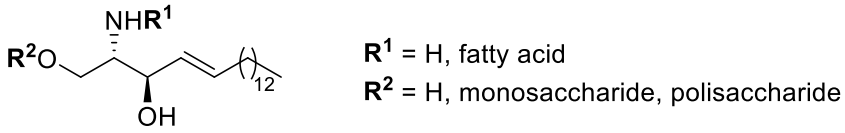

Figure 1: General structure of sphingolipids

Although sphingolipids were initially studied due to their function as the main components of cell membranes, this work will give special relevance to their regulatory capacity on cell proliferation emerging from the balance between three specific sphingolipids: ceramide, sphingosine, and sphingosine-1-phosphate. This balance is called sphingolipid rheostat (Scheme 1).[3]

Because the sphingolipid metabolism entirely consists of enzyme-catalysed reversible reactions, it can be said that exists a continuous flow of transformations that alter cell survival by changing concentrations of metabolites that promote or deny apoptosis. Specifically, several studies

[1] Thudichum, J.L.W.*A Treatise on the Chemical Constitution of the Brain*; Archon Books: North Haven, CT, USA, **1962**.
[2] Tirodkar, T. S.; Voelkel-Johnson, C. Sphingolipids in Apoptosis. *Exp. Oncol.* **2012**, *34*, 231–242.
[3] Ogretmen, B.; Hannun Y.A. Biologically active sphingolipids in cancer pathogenesis and treatment. *Nat Rev. Cancer.* **2004**, *4*, 604-616.

directly link the presence of high concentrations of ceramide with high rates of apoptosis while sphingosine-1-phosphate would present an antagonistic effect, promoting cell survival.[4, 5]

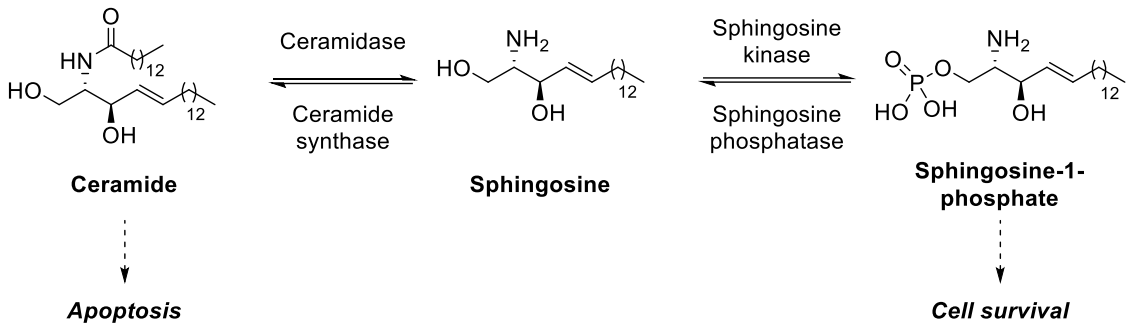

Scheme 1: Sphingolipid rheostat

1.2. *De novo* synthesis of dihydroceramide and Des1

The *de novo* synthesis of ceramide begins with the reaction between serine and palmitoyl-CoA catalysed by serine palmitoyl transferase. Then, the obtained aminoketone is enzymatically reduced by a reductase to give dihydrosphingosine, which in turn is acylated by dihydroceramide synthase to produce dihydroceramide. The last step consists of *E*-configured double bond formation at positions C4-C5, leading to ceramide by the action of dihydroceramide desaturase 1 (Scheme 2).[4, 6]

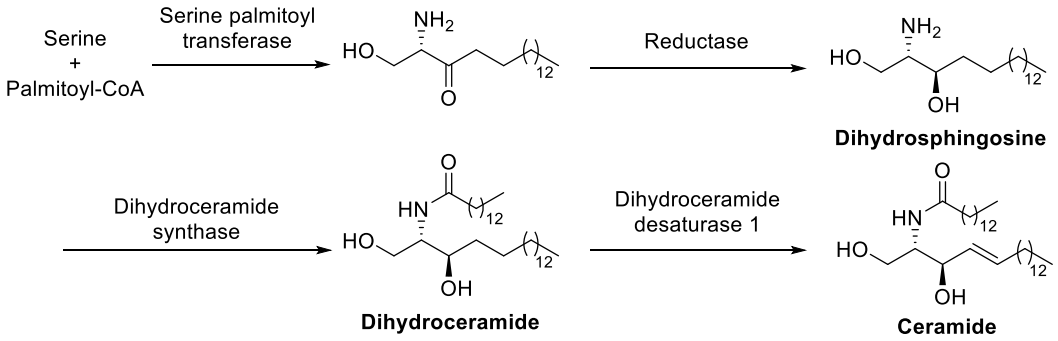

Scheme 2: De novo synthesis of ceramide

[4] Morad, S. A. F.; Cabot, M. C. Ceramide-Orchestrated Signalling in Cancer Cells. *Nat. Rev. Cancer* **2013**, *13*, 51–65.

[5] Kee, T. H.; Vit, P.; Melendez, A. J. J. Sphingosine Kinase Signalling In Immune Cells. *Clin. Exp. Pharmacol. Physiol.* **2005**, 153–161.

[6] Michel, C.; Van Echten-Deckert, G.; Rother, J.; Sandhoff, K.; Wang, E.; Merrill, A. H. Characterization of Ceramide Synthesis. A Dihydroceramide Desaturase Introduces the 4,5-*Trans*-Double Bond of Sphingosine at the Level of Dihydroceramide. *J. Biol. Chem*. **1997**, *272*, 22432–22437.

The turning point in the knowledge of ceramides occurred in 2006, when the advances in sphingolipidomics allowed Merrill *et al.* to observe high presence of dihydroceramide, as well as an unexpectedly low concentration of ceramide, when treating human prostate cells with fenretinide (4-hydroxyphenylretinamide), a known antitumoral product.[7] This observation was crucial, given that until that moment it was believed that dihydroceramide was not biologically active and, in fact, a hypothetical increase in ceramide was considered responsible for the antitumoral efficacy of fenretinide.

This study not only demonstrated that dihydroceramide was biologically active, but it also could participate in the biological rheostat effectively enough to be considered one of the active components in cancer therapy. A new possible target against diseases based on cell proliferation had just been discovered: the enzyme Des1.

Possible functions of dihydroceramide include regulation of oxidative stress, hypoxia, induction of autophagy, regulation of inflammation, reduction of cell proliferation and has been profiled as a molecule with the potential to treat diseases such as cancer, diabetes, inflammation-related diseases, certain neurodegenerative diseases, and AIDS.[8, 9, 10, 11]

Regarding the active centre, it has been suggested that Des1 contains a non-heme dioxo-diiron species as a prosthetic group (Fe_2O_2) that specifically abstracts the C4 hydrogen atom from the dihydroceramide *via* a rate-limiting step to form a very short-lived radical intermediate, which is followed by the fast elimination of a hydrogen atom from C5 to give ceramide.[12]

---

[7] Zheng, W.; Kollmeyer, J.; Symolon, H.; Momin, A.; Munter, E.; Wang, E.; Kelly, S.; Allegood, J. C.; Liu, Y.; Peng, Q.; Ramaraju, H.; Sullards, M. C.; Cabot, M.; Merrill, A. H. Ceramides and Other Bioactive Sphingolipid Backbones in Health and Disease: Lipidomic Analysis, Metabolism and Roles in Membrane Structure, Dynamics, Signaling and Autophagy. *Biochim. Biophys. Acta - Biomembr.* **2006**, *1758*, 1864–1884.

[8] Rodriguez-Cuenca, S.; Barbarroja, N.; Vidal-Puig, A. Dihydroceramide Desaturase 1, the Gatekeeper of Ceramide Induced Lipotoxicity. *Biochim. Biophys. Acta - Mol. Cell Biol. Lipids* **2015**, *1851*, 40–50.

[9] Siddique, M. M.; Li, Y.; Chaurasia, B.; Kaddai, V. A.; Summers, S. A. Dihydroceramides: From Bit Players to Lead Actors. *J. Biol. Chem.* **2015**, *290*, 15371–15379.

[10] Vieira, C. R.; Munoz-Olaya, J. M.; Sot, J.; Jiménez-Baranda, S.; Izquierdo-Useros, N.; Abad, J. L.; Apellániz, B.; Delgado, R.; Martinez-Picado, J.; Alonso, A.; Casas, J.; Nieva, J. L.; Fabriás, G.; Mañes, S.; Goñi, F. M. Dihydrosphingomyelin Impairs HIV-1 Infection by Rigidifying Liquid-Ordered Membrane Domains. *Chem. Biol.* **2010**, *17*, 766–775.

[11] Pullmannova, P.; Maixner, J. Effects of Ceramide and Dihydroceramide Stereochemistry at C-3 on the Phase Behavior and Permeability of Skin Lipid Membranes. *Langmuir.* **2018**, *34*, 521−529.

[12] Fabriàs, G.; Muñoz-Olaya, J.; Cingolani, F.; Signorelli, P.; Casas, J.; Gagliostro, V.; Ghidoni, R. Dihydroceramide Desaturase and Dihydrosphingolipids: Debutant Players in the Sphingolipid Arena. *Prog. Lipid Res*. **2012**, *51*, 82–94.

1.3. Sphingolipid inhibitors of Des1

The first and, to this date, best inhibitor of the enzyme Des1 was described in 2001 by Llebaria *et al*. It is a C_8-cyclopropenyl ceramide, called GT11, and it was the starting point for the creation of some analogues aimed at inhibiting the enzyme Des1.

This ceramide derivative exhibits a competitive dose-dependent enzyme inhibition with a Ki of 6 µM and an IC_{50} of 23 nM, showing activity both *in vitro* and in intact cells. At that time it was suggested that this compound could induce an irreversible inhibition by the reaction of the cyclopropene ring with a cysteine residue of the active site of the enzyme.[13, 14] Nevertheless, the crystal structure of Des1, neither alone nor in complex with an inhibitor, has been experimentally reported yet to confirm this issue. Recent advances in computational science have shed some light on this topic, which will be extensively discussed later in this work.

GT11 analogues bearing urea (**A**, Figure 2), thiourea (**B**, Figure 2) and α-ketoamide moieties (**C**, Figure 2) maintain inhibitory activity, although with less potency, while *N*-methylation of the amide group (**D**, Figure 2) or its replacement by a carbamate (**E**, Figure 2) cause the disappearance of the inhibitory effect.[15]

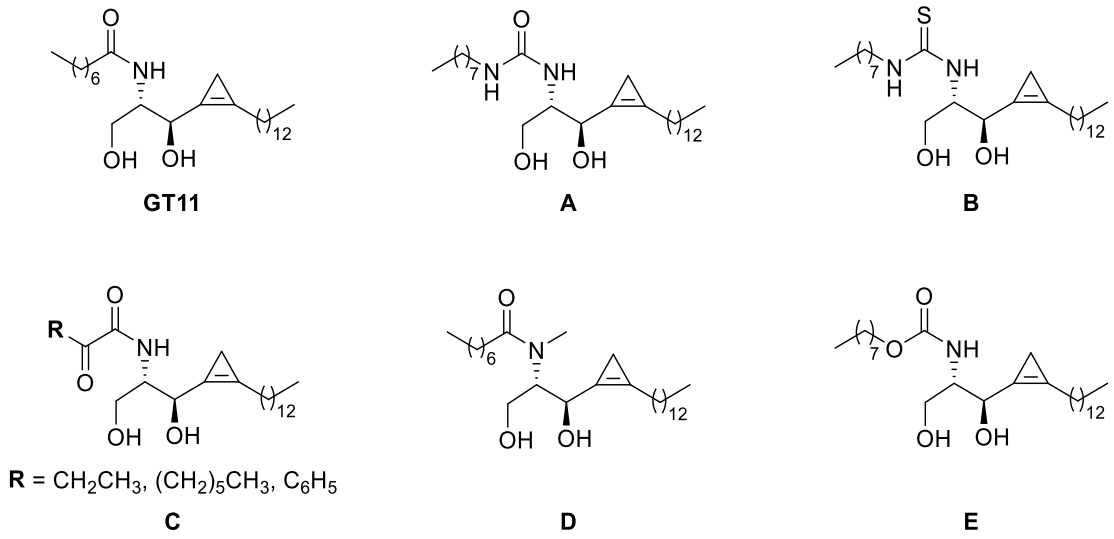

Figure 2: GT11 analogues with N-acyl chain modifications

[13] Triola, G.; Fabriàs, G.; Llebaria, A. Synthesis of a Cyclopropene Analogue of Ceramide, a Potent Inhibitor of Dihydroceramide Desaturase. *Angew. Chem. Int. Ed.* **2001**, *40*, 1960–1962.
[14] Quintana, J.; Barrot, M.; Fabrias, G.; Camps, F. A Model Study on the Mechanism of Inhibition of Fatty Acyl Desaturases by Cyclopropene Fatty Acids. *Tetrahedron* **1998**, *54*, 10187–10198.
[15] Bedia, C.; Llebaria, A. Analogs of the Dihydroceramide Desaturase Inhibitor GT11 Modified at the Amide Function: Synthesis and Biological Activities. *Org. Biomol. Chem.* **2005**, 3707–3712.

In terms of acyl chain length, only GT11 analogues with 6 and 10 carbon atoms retain inhibitory activity with an IC_{50} = 31 μM and 13 μM, respectively (Figure 3). The activity of these acyl chains may be related to cell permeability.[16]

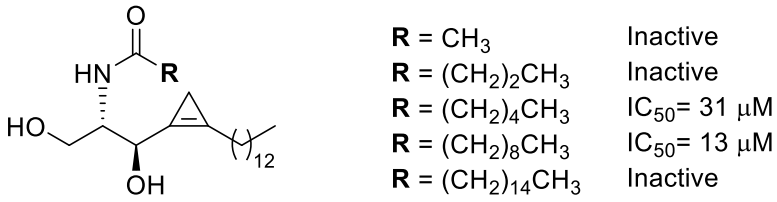

Figure 3: GT11 analogues with N-acyl chain length modifications

Among other ceramide-like Des1 inhibitors described so far, the 5-thiadihydroceramide named XM462 (Figure 4) stands out as one of the most important, inhibiting Des1 both *in vitro* (IC_{50} = 8.2 μM) and in intact cells (IC_{50} = 0.43 μM), at a substrate concentration of 10 μM and in a dose-dependent manner. It has been demonstrated that XM462 is able to induce autophagy in human gastric cancer cell line HG27 by effectively increasing the levels of dihydroceramide.[17]

Other analogues of XM462 (**RBM-1B**, **RBM-1C**, and **RBM-1D**, Figure 4) have also been reported, but none of them proved to be more effective than XM462. This fact suggested that the hydroxyl group at C3 could be a requirement for high inhibitory activities.[18]

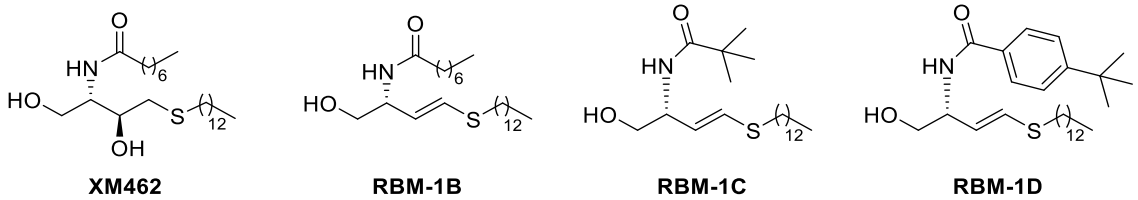

Figure 4: XM462 and its analogues

[16] Triola, G.; Fabriàs, G.; Casas, J.; Llebaria, A. Synthesis of Cyclopropene Analogues of Ceramide and Their Effect on Dihydroceramide Desaturase. *J. Org. Chem.* **2003**, *68*, 9924–9932.

[17] Muñoz-Olaya, J., Matabosch, X., Bedia, C., Egido-Gabás, M., Casas, J., Llebaria, A., Delgado, A., Fabriàs, G. Synthesis and Biological Activity of a Novel Inhibitor of Dihydroceramide Desaturase. *ChemMedChem* **2008**, *3*, 946 – 953.

[18] Camacho, L.; Simbari, F.; Garrido, M.; Luis, J.; Casas, J.; Delgado, A.; Fabriàs, G. 3-Deoxy-3, 4-Dehydro Analogs of XM462. Preparation and Activity on Sphingolipid Metabolism and Cell Fate. *Bioorg. Med. Chem*. **2012**, *20*, 3173–3179.

1.4. Novel ceramide analogues synthesized in SINTCARB research group

Structure-activity studies involve an iterative work in which structural changes are applied to an initial molecule to discern how they affect biological properties. In this sense, and thanks to the information provided by the sphingolipid-based inhibitors of the Des1 described to this date and the synthesis of new analogues, a better understanding about how the Des1 enzyme works and, therefore, to gradually limit the characteristics that should present an ideal candidate for inhibition can be reached.

In this regard, in the SINTCARB research group a series of potential Des1 inhibitors were synthesized. These compounds contained all known requirements for inhibition with structural changes aimed at gathering more information towards the design of a Des1 inhibitor. These requirements are:

- A 2,3-aminoalcohol moiety in *anti*-disposition, concretely, *2*S,*3*R.
- A free hydroxyl group at C1.
- A non-modified amide moiety.

The first family of potential inhibitors consisted of a 1,4-disubstituted 1,2,3-triazole group[19] (Figure 5, **S1**) and a 1,5-disubstituted 1,2,3-triazole group[20] (Figure 5, **S2**) as cores since they can mimic the conformational constraint imposed on alkyl chains by a double bond acting, in this sense, as an olefinomimetic element. Besides, the presence of 1,2,3-triazole group was expected to increase the binding of these substrates with Des1 by the formation of π-π stacking interactions and/or additional dipole-dipole interactions, due to the capacity of the N2 and N3 electron lone pairs to serve as hydrogen bond acceptors, chelating units and/or performing *N*-oxidation.[21, 22] Moreover, because of the strong dipole moment of triazoles (approximately 5 Debye, larger than that of the amide group), the C-H bond from the triazole is polarized and can

[19] Martí Torrell, C. Synthesis of potential dihydroceramide desaturase 1 inhibitors based on triazole motifs as a therapeutical target against cancer. Master Thesis, Universitat Rovira i Virgili (SINTCARB), 2018.
[20] Rivero Prieto, P. Ph.D. student at SINTCARB research group.
[21] Appendino, G.; Bacchiega, S.; Minassi, A.; Cascio, M. G.; De Petrocellis, L.; Di Marzo, V. The 1,2,3-Triazole Ring as a Peptido- and Olefinomimetic Element: Discovery of Click Vanilloids and Cannabinoids. *Angew. Chem. Int. Ed*. **2007**, *119*, 9312-9315.
[22] Pagliai, F.; Pirali, T.; Del Grosso, E.; Di Brisco, R.; Tron, G.C.; Sorba, G.; Genazzani, A. A. Rapid Synthesis of Triazole-Modified Resveratrol Analogues via Click Chemistry. *J. Med. Chem.* **2006**, *49*, 467-470.

act as a hydrogen-bond donor, allowing interactions with neighbouring carbonyl groups of the protein. In addition, it could present less frequent interactions such as C-H···π.[23, 24]

Furthermore, at the time it was thought that Des1 inhibition could be an irreversible process by reaction of the cyclopropene ring of GT11 with a cysteine residue of the desaturase active centre. A 1,2,3-triazole unit could partially mimic the rigid backbone of cyclopropene moiety. However, unlike the cyclopropene double bond, the triazole double bond is involved in aromatic stabilization and a different reactivity would be expected. Thus, results of biological assays from these triazole derivatives could also bring light to the inhibition mechanism of this enzyme.[25]

Another explored core was the 1,4-disubstituted furan[20] (Figure 5, **S3**). Being a heterocyclic aromatic ring, furans are also able to display most of the interactions present in triazoles, such as π -π stacking interactions and the ability to act as a hydrogen bond acceptor. The presence of the oxygen atom was expected to be beneficial towards a possible chelation and, additionally, the furan ring could undergo ring oxidation.[26]

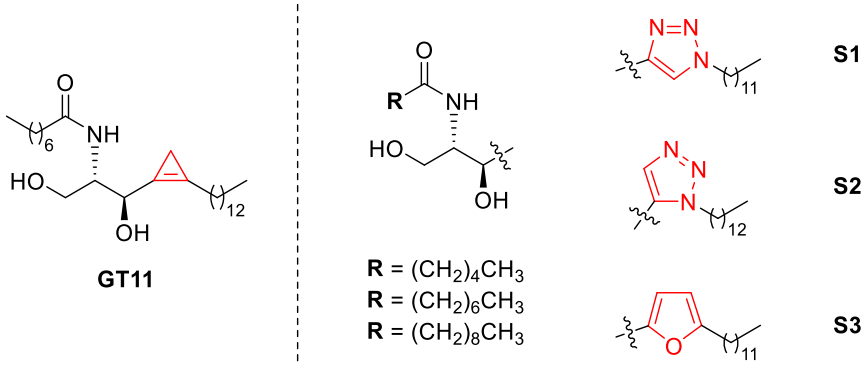

Figure 5: Structural comparison between GT11 and novel ceramide analogues synthetized in SINTCARB research group. Structural modifications related to the central core are highlighted in red.

Triazole derivatives caused a statistically significant Des1 inhibition in intact cells (20-30%), but a lack of activity was observed in lysates. In the case of furan-based analogues the inhibition reached a 45% in the case of the compound bearing a *N*-acyl chain of 6 carbons. These results

[23] Massarotti, A.; Aprile, S.; Mercalli, V.; Grosso, E. Del; Grosa, G.; Sorba, G.; Cesare, G. Are 1,4- and 1,5-Disubstituted 1,2,3-Triazoles Good Pharmacophoric Groups? *ChemMedChem* **2014**, 2497–2508.
[24] Agalave, S. G.; Maujan, S. R.; Pore, V. S. Click Chemistry: 1,2,3-Triazoles as Pharmacophores. *Chem. An Asian J*. **2011**, *6*, 2696–2718.
[25] Brik, A.; Alexandratos, J.; Lin, Y.-C.; Elder, J. H.; Olson, A. J.; Wlodawer, A.; Goodsell, D. S.; Wong, C.-H. 1,2,3-Triazole as a Peptide Surrogate in the Rapid Synthesis of HIV-1 Protease Inhibitors. *ChemBioChem* **2005**, *6*, 1167-1169.
[26] Peterson, L. A. Reactive Metabolites in the Biotransformation of Molecules Containing a Furan Ring. *Chem. Res. Toxicol*. **2013**, *26*, 6–25.

could indicate that the presented analogues may not affect directly to the enzyme active site but the electron transport chain instead. This hypothesis is currently being studied.

1.5. Artificial intelligence for protein folding and docking studies

According to Levinthal's paradox, even though a single protein has a massive number of possible conformations it folds in milli, and even microseconds. Therefore, there must be local interactions that speed up the process, which suggests that the amino acid sequence could be the key to protein folding.[27] This has become one of the pillars of the theory of protein folding, which led to the creation of protein structure prediction programs such as AlphaFold 2.

AlphaFold 2 is a software developed by DeepMind (Google) and EMBL-EBI that focuses on the use of artificial intelligence to generate 3D protein structures from its aminoacid sequence powered by a state-of-the-art system of deep learning based on 170000 proteins with known aminoacid sequence and structure. It has been disclosed as an open-source software.

The average error of this program was evaluated by the Global Distance Test (GDT), which is a metric that ranges from 0 to 100 and can be approximately thought of as the percentage of aminoacid residues within a threshold distance from the correct position. It is informally considered that results over 90 are competitive with experimental methods. AlphaFold 2 achieves an average of 92.4 GDT, which translates to an average error of only 1.6 Å.[28]

On 21st of July 2021 AlphaFold 2 released high-quality predictions for the 3D shape of every single protein in the human body, which included Des1,[29] causing massive scientific excitement. To put it in perspective, the publication of this work more than doubled humanity's accumulated knowledge of high-accuracy human protein structures.[30] It has been regarded as one of the most important datasets since the mapping of the human genome and it is expected to accelerate scientific knowledge to a great extent.

---

[27] Zwanzig, R.; Szabo, A.; Bagchi, B. Levinthal's Paradox. *Proc. Nail. Acad. Sci.* **1992**, *89*, 20–22.

[28] Schauperl, M.; Denny, R. A. AI-Based Protein Structure Prediction in Drug Discovery: Impacts and Challenges. *J. Chem. Inf. Model.* **2022***, 62,* 3142–3156.

[29] AlphaFold Protein Structure Database, Des1. https://alphafold.ebi.ac.uk/entry/O15121 (accessed 11 July 2022).

[30] Jumper, J.; Evans, R.; Pritzel, A.; Green, T.; Figurnov, M.; Ronneberger, O.; Tunyasuvunakool, K.; Bates, R.; Žídek, A.; Potapenko, A.; Bridgland, A.; Meyer, C.; Kohl, S. A. A.; Ballard, A. J.; Cowie, A.; Romera Paredes, B.; Nikolov, S.; Jain, R.; Adler, J.; Back, T.; Petersen, S.; Reiman, D.; Clancy, E.; Zielinski, M.; Steinegger, M.; Pacholska, M.; Berghammer, T.; Bodenstein, S.; Silver, D.; Vinyals, O.; Senior, A. W.; Kavukcuoglu, K.; Kohli, P.; Hassabis, D. Highly Accurate Protein Structure Prediction with AlphaFold. *Nature* **2021**, *596*, 583–589.

Spurred by the very confident 3D structure prediction provided by AlphaFold 2 for Des1, a collaborative project with Dr. Xavier Barril (UB)[31] was recently initiated. In the frame of this collaboration, this powerful tool is being used to shed some light on the inhibition mode of this enzyme through the study of the topology of the binding site and the location of the diiron prosthetic group of Des1.

Since Alpha Fold 2 only provides the aminoacid structure, the non-heme dioxo-diiron group had to be introduced manually by Dr. Barril's research group. It was positioned at the end of a well-defined deep pocked where one iron atom is being coordinated by 5 histidine residues and the second one by 4 histidine and 1 glutamine residues (Figure 6).

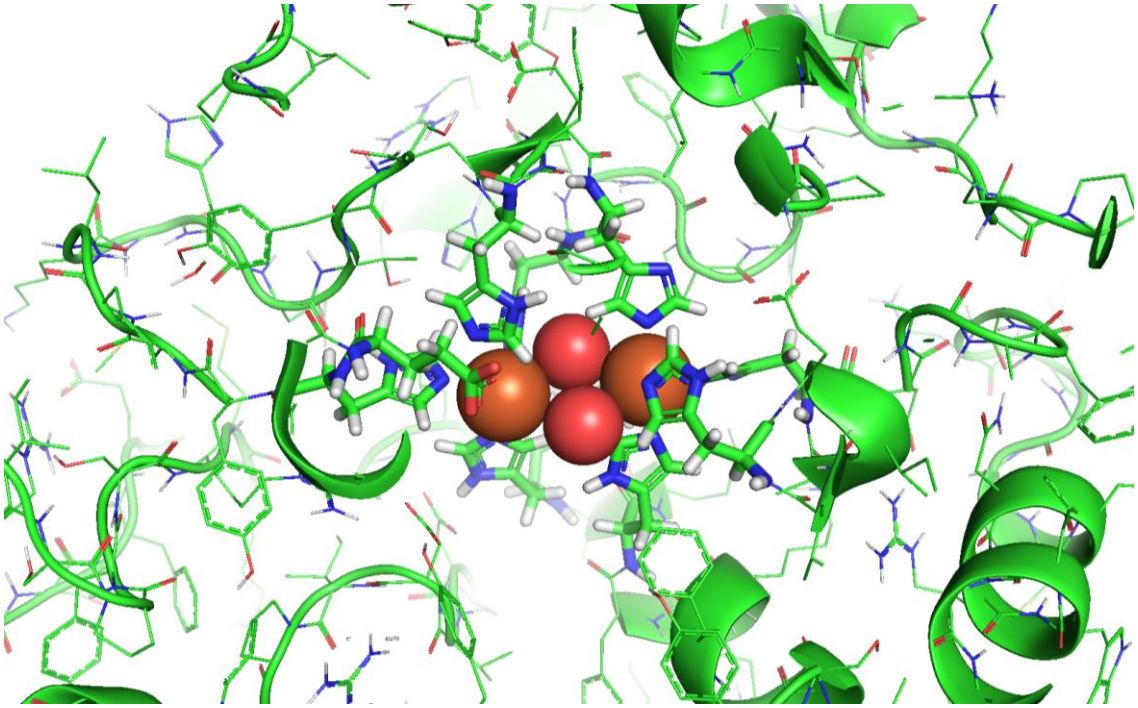

Figure 6: Representation of Des 1 with the non-heme dioxo-diiron specie

Preliminary docking studies with recognized Des1 inhibitors, concretely GT11 (Figure 7, left) and XM462 (Figure 7, right), to envisage preferred conformations of the ligands in the binding site, determine residues present at the contact surface and, especially, surrounding the diiron species prosthetic group were done in our group.

[31] Dr. Xavier Barril Alonso. Dept. Pharmacy and Pharmaceutical Technology and Physical Chemistry, Faculty of Pharmacy and Food Sciences, University of Barcelona.

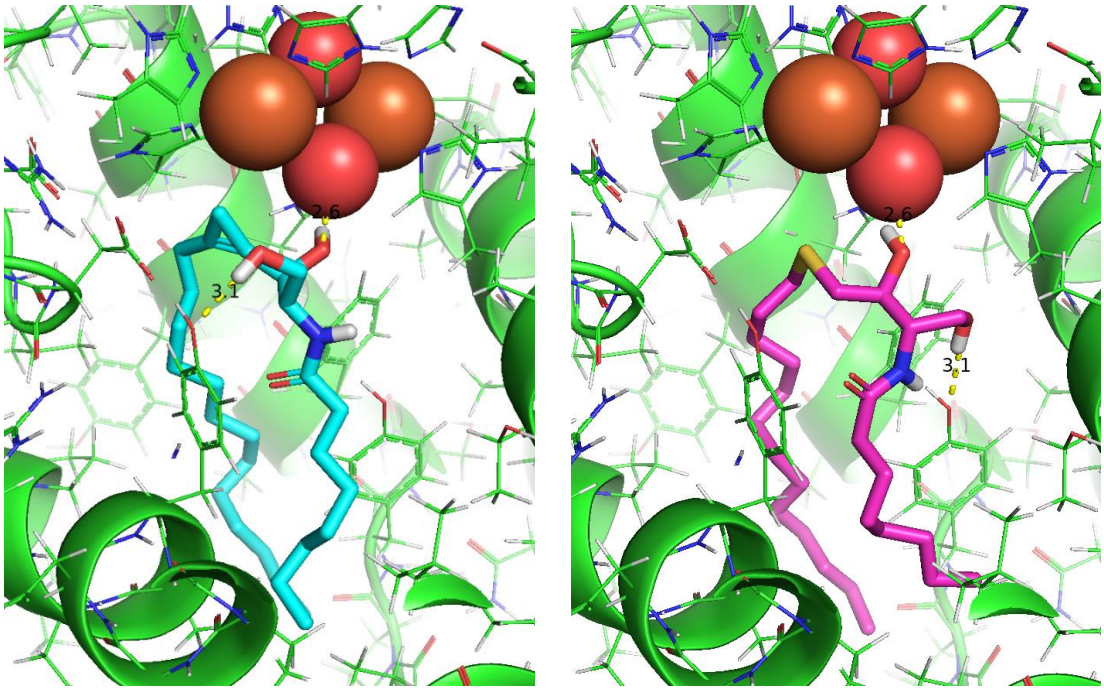

Figure 7: Preferred conformations of GT11 (left) and XM462 (right) in Des1 active site

As it can be seen, the best scoring binding mode for the GT11 showed a bifolded conformation of the hydrophobic tails of the compound resulting in the proximity of the cyclopropylene ring to one of the iron metal centres. Following this arrangement in the binding pocket, the C3 hydroxyl group formed a hydrogen bond with the oxygen from the dioxo-diiron complex while the C1 hydroxyl group participated in a hydrogen bond with Tyr170.

In the case of compound XM462, the best docking pose showed the same hydrogen bond interaction between the oxygen from the complex and C3 hydroxyl group and the sulphur atom close to the same iron metal centre with the hydrophobic tails also in a bifolded conformation. Additionally, the C1 hydroxyl group formed a hydrogen bond with Tyr120.

These preliminary studies have shown that there are no cysteines nearby the Des1 active centre, as was originally believed. Thus, any approach that implies an irreversible inhibition *via* reaction with cysteine residues could be discarded.

Importantly, docking studies also shed light in the inhibitory activity displayed by the previous synthetized ceramide analogues in SINTCARB research group.

In the case of the 1,2,3-triazole family it was noticed that the size of the ring moiety affected the folding of the structure. In the case of **S1**, the arrangement of the hydroxyl groups changed, leading to a loss of favourable hydrogen bond interactions, and increasing the distance between

the core and the active centre (Figure 8, left). In comparison, the ring head of compound **S2** was able to get closer to the iron metal centre and allowed the structure to fold properly (Figure 8, right). The position of the ring allowed the formation of the hydrogen bond between the C3 hydroxyl group and the dioxo-diiron oxygen atom of the active centre. The hydrogen bond interaction between the C1 hydroxyl group and Tyr170 was not formed, possibly due to the ring's size or even its nature. Nevertheless, the hydroxyl group was able to establish an intramolecular hydrogen bond with the C3 hydroxyl group.

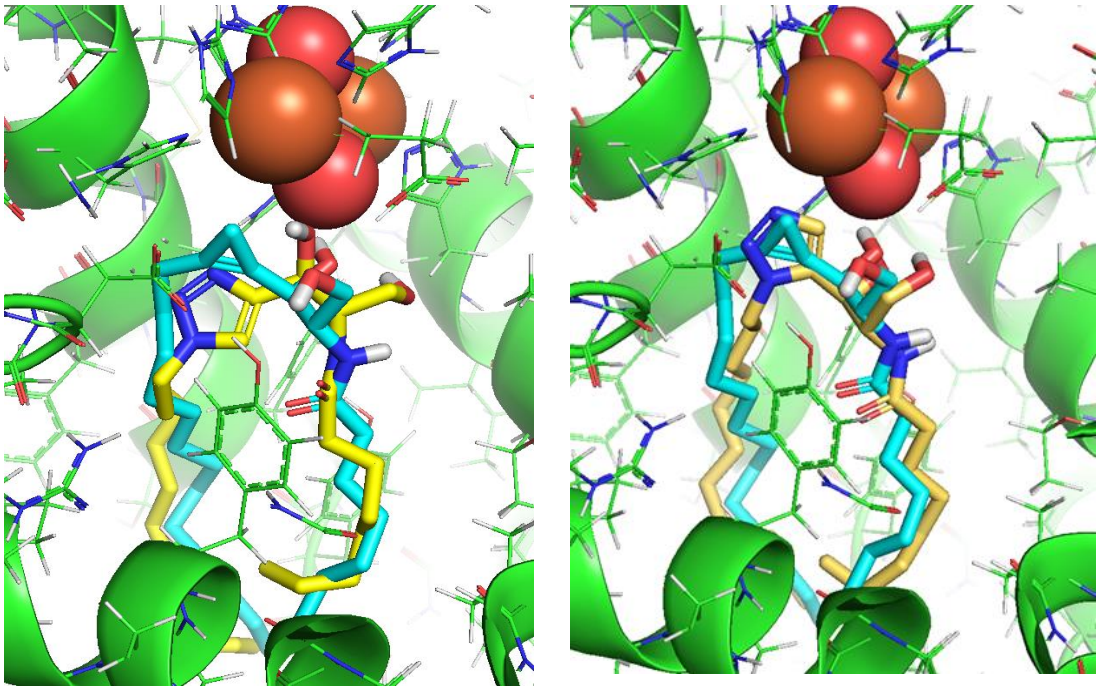

*Figure 8: Preferred conformation of compounds **S1** (left) and **S2** (right) superposed to the one displayed by GT11*

Regarding compound **S3**, docking studies showed that, even though it displayed the bifolded conformation, both hydroxyl groups were unable to form favourable interactions, again due to the different arrangement of the heterocycle. Moreover, the oxygen atom present in the furan ring was not pointing towards the active centre (Figure 9).

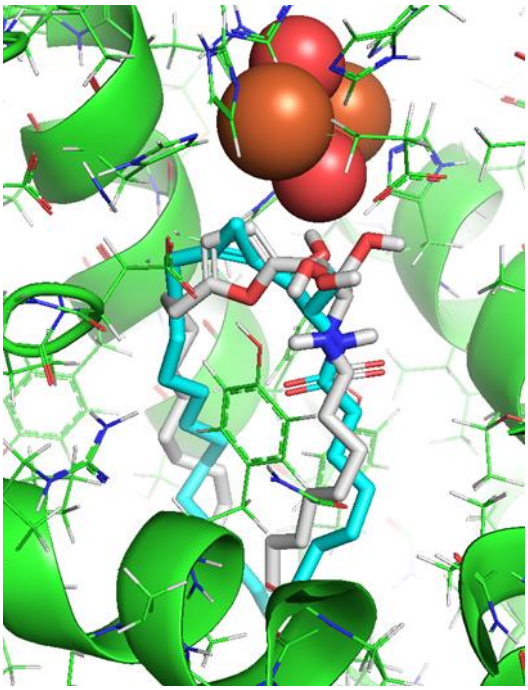

*Figure 9: Preferred conformation of compound **S3** superposed to the one displayed by GT11*

The comparison between the preferred conformations and interactions displayed by GT11, XM462 and the previously synthetized analogues in SINTCARB research group allowed to acquire new possible requirements for inhibitory activity that will be taken into account in this master thesis work. These requirements are:

- The analogue should adopt a bifolded conformation at the active site.
- The heterocycle should be proximal to one of the iron atoms present in the non-heme dioxo-diiron specie.
- C3-OH should perform a hydrogen bond with one of the oxygen atoms present in the non-heme dioxo-diiron specie.
- C1-OH should perform a hydrogen bond with an aminoacid of the enzyme binding site that would allow for a correct conformation of the compound, as well as an effective interaction.

2. Objectives of the work

In this context, the main objective of this master thesis work is the stereoselective synthesis of three ceramide analogues that would be able to inactivate the putative diiron oxidant involved in ceramide double bond formation (Figure 10). All targeted analogues would be evaluated as Des1 inhibitors and, by doing so, a better understanding of the Des1 active site and its inhibition mechanism could be acquired.

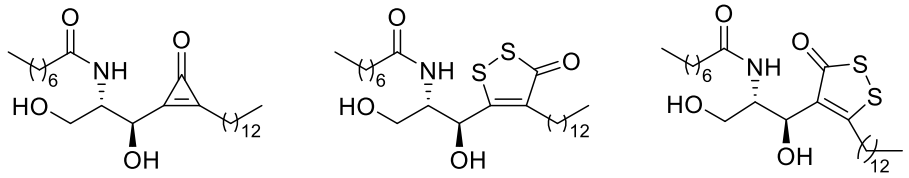

Figure 10: Targeted ceramide analogues

2.1. Justification of the targeted molecules. Docking studies.

The proposed analogues will contain all known requirements for Des1 inhibition, previously mentioned. Furthermore, the *N*-acylated carbon chain will consist of 8 carbons, which is the chain length that currently displays the best inhibitory activity in other analogues. The aliphatic chain will also be the one featured by GT11.

Regarding the core of compound **1**, a cyclopropenone is a highly strained three-membered ring stabilized by aromaticity, being the unusual case in Hückel's rule where N = 0.

Cyclopropenones are electrophilic and may undergo 1,2- or 1,4-addition reactions, a property that has been taken advantage of in the past to irreversibly inhibit proteinases that contained cysteine or serine residues at the active site of enzyme.[32] Also, they can be used as a reversible inhibitor of the targeted enzyme or receptor. Moreover, cyclopropenones are stable in biological medium and, in fact, there are examples of drugs already featuring this moiety, such as the antibiotic Penitricin.[33]

Even though there are no cysteines in the active site of Des1, the use of a cyclopropenone core it is highly desirable since its geometry is expected to directly point its carbonyl group towards

[32] Ando, R.; Sakaki, T.; Morinaka, Y.; Takahashi, C.; Tamao, Y.; Yoshii, N.; Katayama, S.; Saito, K. I.; Tokuyama, H.; Isaka, M.; Nakamura, E. Cyclopropenone-Containing Cysteine Proteinase Inhibitors. Synthesis and Enzyme Inhibitory Activities. *Bioorganic Med. Chem*. **1999**, *7*, 571–579.
[33] Tokuyama, H.; Isaka, M.; Nakamura, E.; Ando, R.; Morinaka, Y. Synthesis And Biological Activities Of Cyclopropenone Antibiotic Penitricin And Congeners *J. Antibiot*. **1992**, *45*, 1148-1154.

the active site of the Des1, and therefore it could inactivate the enzyme *via* coordination with one of the iron atoms, responsible for the biological activity.

This approach is supported by docking studies of the targeted molecule **1**. It was revealed that the cyclopropenone head in the structure would be placed near the iron metal centre and help the proper arrangement of the other functional groups. The most probable binding mode showed that the C3 hydroxyl group could interact with the dioxo-diiron oxygen while the C1 hydroxyl group would form a hydrogen bond with Glu232. This preferred conformation is remarkably similar to the displayed by GT11 (Figure 11).

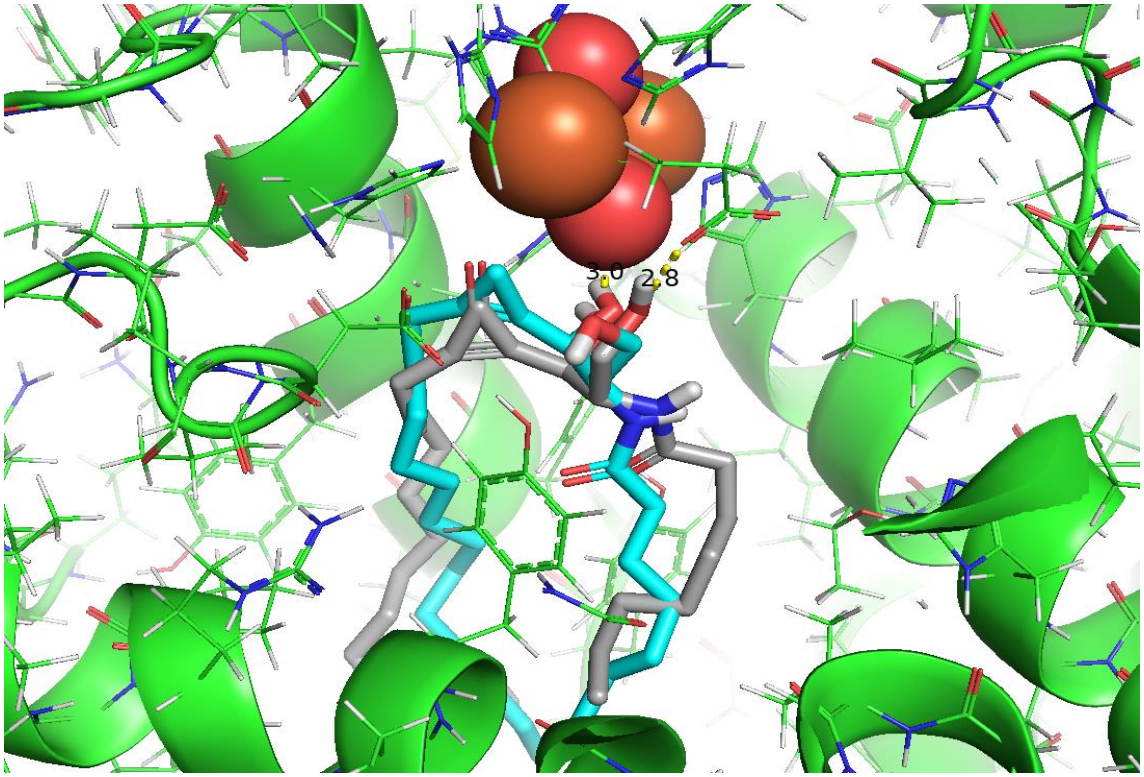

*Figure 11: Preferred conformation of the targeted ceramide analogue **1** (grey) superposed to the one displayed by GT11 (blue)*

Additionally, two new ceramide analogues bearing a 1,2-dichalcogen heterocycle, **2** and **3**, could be synthetized with only one late-stage functionalization step by harnessing the singular reactivity of cyclopropenones.[34]

1,2-Dichalcogen heterocycles represent an important class of heterocycles due to their significant pharmacological activities, which include but are not limited to: chemotherapy,

[34] Wu, J.; Gao, W.; Huang, X.; Zhou, Y.; Liu, M.; Wu, H. Selective [3+2] Cycloaddition of Cyclopropenone Derivatives and Elemental Chalcogens. *Org. Lett.* **2020**, *22*, 5555−5560.

antioxidant, and radiation protection agents. This family of heterocycles have also been used as chemopreventive, choleretic, and sialagogue agents in various biomodels.[35, 36] In our case, the introduction of sulphur atoms to the molecule is especially desirable since it has already been reported the inhibition of different enzymes via sulphur coordination of the non-heme oxo species. Concretely it was the case of ETHE1, a member of a growing subclass of nonheme iron enzymes that catalyses the deoxygenation of glutathione persulfide to glutathione.[37]

Docking studies showed that the geometry of the ceramide analogue **2** is not only useful towards this approach, but the overall interactions would deem it as a potential Des1 inhibitor. Notably, the sulphur atoms in the ring could coordinate one of the irons in the complex catalytic site. Moreover, the hydroxyl group located at C3 forms a hydrogen bond with the dioxo-diiron oxygen, similar to the case of GT11. Regarding other interactions also present in GT11, in the case of compound **2** the C1 hydroxyl group is losing its interaction with Tyr170, probably due to steric effects from the bulkier ring. On the other hand, a hydrogen bond interaction appears between the nitrogen in compound **2** and Tyr170. As a result, the carbonyl group situated downward on the tail forms a hydrogen bond with residue Tyr120 (Figure 12, left).

Regarding ceramide analogue **3**, docking studies indicated that the sulphur atoms in the hetero ring could again coordinate one of the iron atoms in the complex catalytic site. It was noticed that due to the increase in steric hindrance at the polar head the carbonyl and hydroxyl groups change orientations in the pocket, leading to different interactions with key residues. The hydrogen bond between the C3 hydroxyl group and the dioxo-diiron oxygen is kept as with GT11. On the other hand, the C1 hydroxyl group is losing its interaction with Tyr170 due to the different position of the ring head. As a result of the pushed shorter tail, the carbonyl group situated downward on the tail forms a hydrogen bond with residue Tyr120 (Figure 12, right).

[35] Smith, A. W.; Arif, J. M.; Gupta, R. C. 1,2-Dithiole-3-thioneand its Structural Analogue Oltipraz are Potent Inhibitors of Dibenzo[a,1]pyrene-DNA Adduction in Female Sprague-Dawley Rats. *Int. J. Cancer* **2001**, *91*, 132−136.

[36] Drukarch, B.; Schepens, E.; Stoof, J. C.; Langeveld, C. H. Anethole Dithiolethione Prevents Oxidative Damage in Glutathione-Depleted Astrocytes*. Eur. J. Pharmacol*. **1997**, *329*, 259−262.

[37] Goudarzi, S.; Babicz, J. T.; Kabil, O.; Banerjee, R.; Solomon, E. I. Spectroscopic and Electronic Structure Study of ETHE1: Elucidating the Factors Influencing Sulfur Oxidation and Oxygenation in Mononuclear Nonheme Iron Enzymes. *J. Am. Chem. Soc*. **2018**, *140*, 14887−14902.

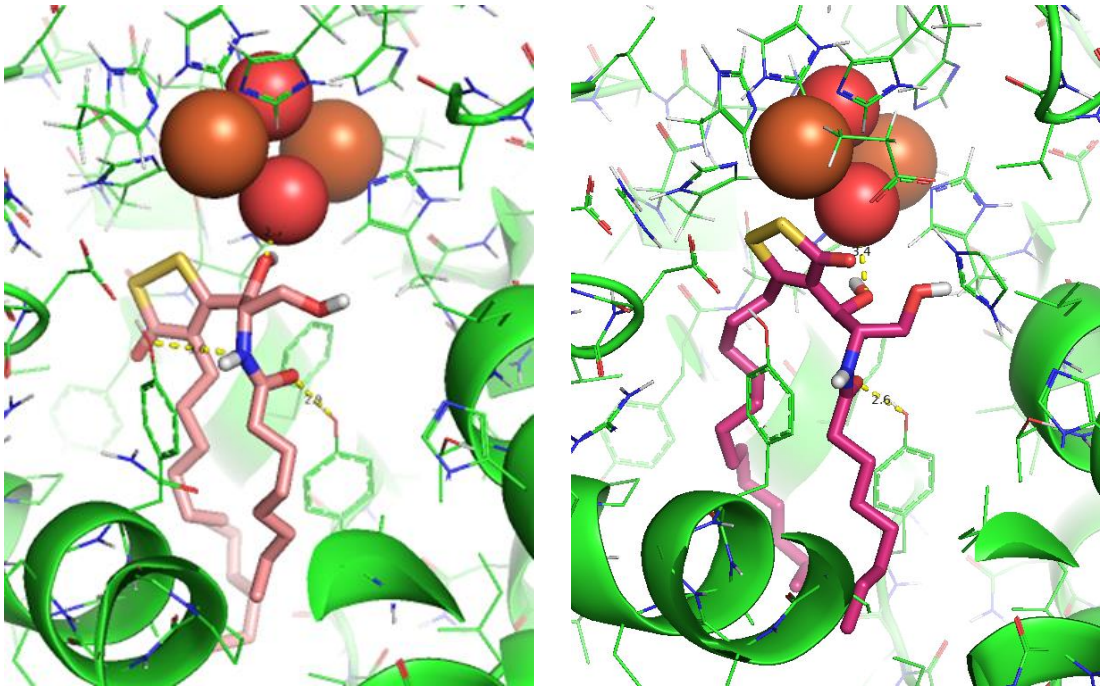

*Figure 12: Preferred conformation of targeted ceramide analogues **2** (left) and **3** (right)*

With all this information in mind, the synthesis could be started.

3. Results and discussion

3.1. Initial approach

Originally, it was planned to obtain the targeted analogue **1** from an *N*-acylation of aminodiol **4**, generated from compound **5** by deprotection and concomitant hydrolysis of the difluorocyclopropene unit. The aforementioned moiety should be generated by the electrophilic addition of a difluorocarbene to alkyne **6**, which in turn, can be obtained *via* stereoselective addition of lithium pentadecyn-1-ide to (*S*)-Garner's Aldehyde (Scheme 3).

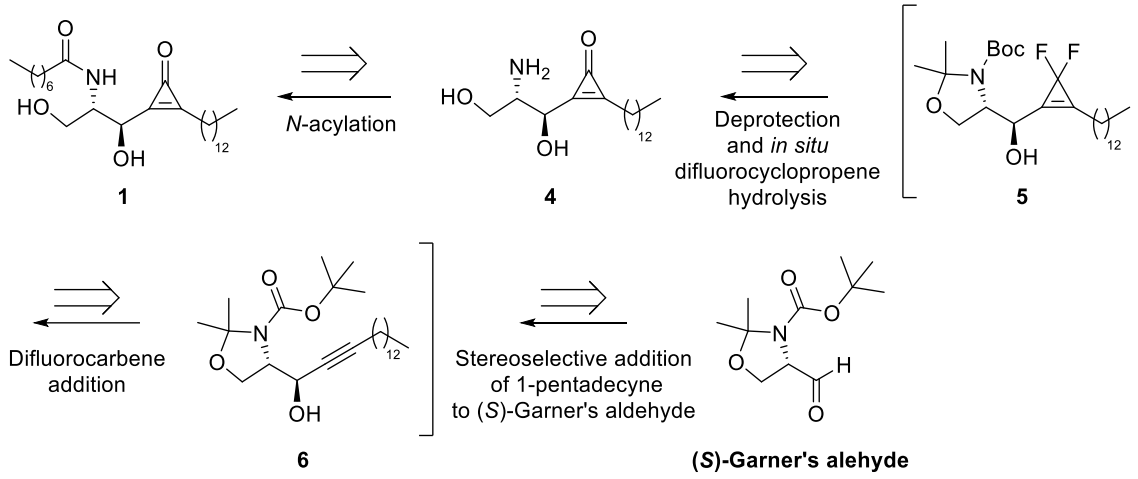

Scheme 3: Retrosynthetic analysis of the initial approach

The synthesis of ceramide-like molecules has been extensively studied in the research group in which this work was developed, and thus, some crucial insights were provided:

- The use of Garner's aldehyde as chiral building block is very effective to attain the 2-amino-1,3-diol functionality with the desired *anti* configuration.[19, 20]
- The difluorocarbene addition and further hydrolysis towards cyclopropenone unit has already been performed in SINCARB research group to a product structurally similar to compound **6**, in a synthesis targeting an enigmol analogue.[38]
- Product **6** cannot be purified by flash column chromatography due to decomposition and must be used as a crude in the next step.[39]

[38] Saltó de la Torre, J. Synthesis of non-fluorinated and fluorinated cyclopropane analogs of enigmol. Master Thesis, Universitat Rovira i Virgili (SINTCARB), 2016.
[39] García, D. Synthesis of potential dihydroceramide desaturase 1 inhibitors as a therapeutical target against cancer. Master Thesis, Universitat Rovira i Virgili (SINTCARB), 2020.

The presented retrosynthetic strategy would allow for the simultaneous deprotection and concomitant *in situ* formation of the ketone. This, in conjunction with not isolating products **5** and **6**, but using the crude instead, would allow obtaining the desired product in an efficient time-saving manner.

The first step of the synthesis involves obtaining the key (2*S*, 3*R*)-2-amino-1,3-diol functionality through the nucleophilic attack of lithium pentadecyn-1-ide onto the carbonyl of (*S*)-Garner's aldehyde, a notable compound of the chiral pool, widely used for this purpose.[40]

Is important to notice that in this nucleophilic addition two different diastereomers can be obtained depending on the face of the carbonyl group on which the attack is performed, determined by the preferred conformation of the transition state.

According to the proposed models to explain this type of addition, the most voluminous substituent attached to the stereogenic centre in α-position to the carbonyl group, namely the *N*-protected group (NPg), is placed orthogonally to the carbonyl group. Then, the nucleophile will approach at the Bürgi-Dunitz angle (105 º) concerning the plane of the carbonyl group, *antiperiplanar* to the bulky group and by the face that presents a minor steric hindrance.[41]

Taking into account these considerations, two possible events can be predicted as a function of the preferred conformation in each case (Figure 13):

- An oxophilic metal (e.g. Zn or Mg) coordinates the carbonyl group of the aldehyde and the nitrogen or the nitrogen's protecting group, in this case being a carbamate, to form a chelate: *Si* face is the least hindered and therefore the final product will present the *syn* stereochemistry. This transition state is called Cram chelate.

- The carbonyl groups are not coordinated: the NPg group is positioned perpendicular to the carbonyl axis due to favourable n-π* interactions from the nitrogen lone pair of electrons. Therefore, *Re* face is the least hindered and the resulting product will present *anti* stereochemistry. This non-chelating transition state is called Felkin-Ahn.

[40] Passiniemi, M.; Koskinen, A. M. P. Garner's Aldehyde as a Versatile Intermediate in the Synthesis of Enantiopure Natural Products. *Beilstein J. Org. Chem.* **2013**, *9*, 2641–2659.
[41] Karjalainen, O. K.; Koskinen, A. M. P. Diastereoselective Synthesis of Vicinal Amino Alcohols. *Org. Biomol. Chem.*, **2012**, *10*, 4311–4326.

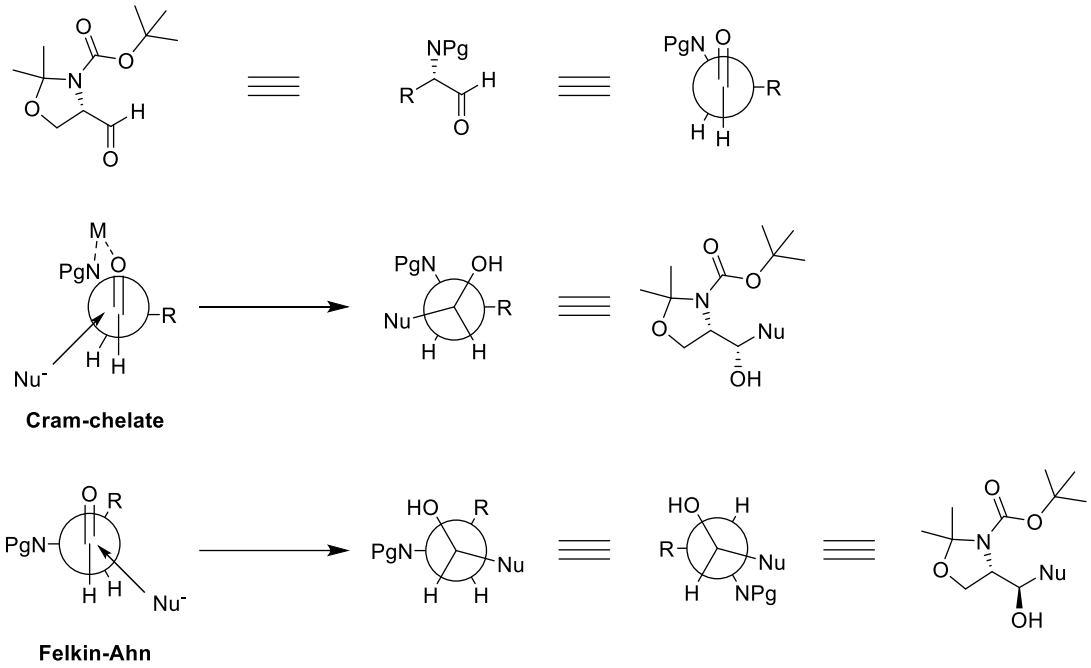

Figure 13: The preferred conformation of the transition state determines the final stereochemistry

To increase the reactivity, hexamethylphosphorotriamide (HMPA) was added as it effectively breaks the lithium clusters by coordinating with this cation, increasing the nucleophilicity of the alkyn-1-ide and promoting the formation of the kinetic *anti*-product.[42, 43]

Temperature control is also essential in order to obtain good stereoselectivity, as demonstrated by Lam's research group in the synthesis of sphingosine analogues. Thus, they obtained a *syn*/*anti* ratio of 1:9 at -50 °C using 1.16 equivalents of BuLi, while above 15 °C and, regardless of the concentration of BuLi, only the *syn* product was observed. This can be explained by the fact that at high temperatures the nucleophilic addition takes place through a thermodynamic transition state that is very similar to the Cram-chelate.[44]

Taking into account these considerations, the reaction was carried out by using both HMPA and at -55 °C to maximize the ratio of the desired *anti* diastereomer. NMR analysis of the reaction crude revealed the *anti* configuration as the only diastereomer.

[42] Herold, P. Synthesis of D-*erythro*- and D-*threo*-Sphingosine Derivatives from L-Serine. *Helvetica Chimica Acta.* **1988**, *71*, 354-362.
[43] Gooch, J. W. Hexamethylphosphoric Triamide. *Encycl. Dict. Polym.* **2011**, 366–366.
[44] Wong, L.; Tan, S. S. L.; Lam, Y.; Melendez, A. J. Synthesis and Evaluation of Sphingosine Analogues as Inhibitors of Sphingosine Kinases. *J. Med. Chem.* **2009**, *52*, 3618–3626.

The crude was not purified due to the reasons commented before. Thus, it was directly used in the subsequent [2+1] cycloaddition to obtain difluorocyclopropene **5** using trifluoromethyltrimethylsilane as difluorocarbene source.[45]

The cyclopropenone formation can be rationalized by the initial release of a fluoride ion that will result in the formation of the aromatic fluorocyclopropenyl cation, which can react with a water molecule. Then, and after a HF elimination, the cyclopropenone would be formed (Scheme 4).[46]

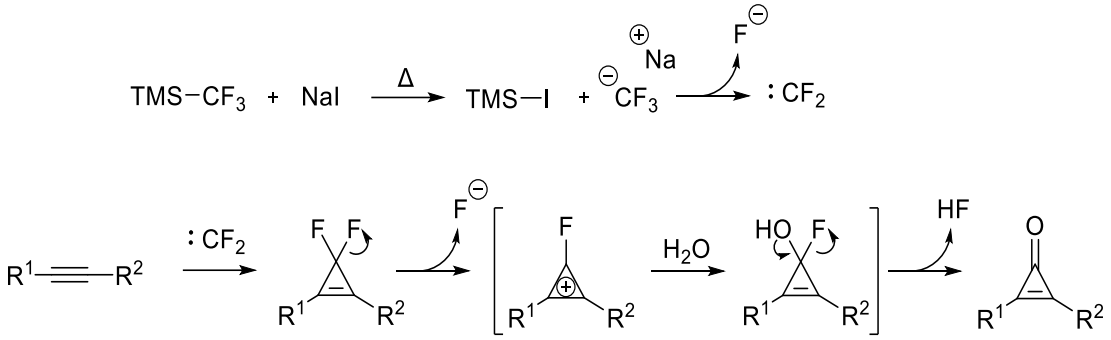

Scheme 4: Difluorocyclopropene and cyclopropenone formation

Difluorocyclopropene products cannot be isolated due to their fast hydrolysis towards its cyclopropenone derivative, prompted by silica purification or even by dissolution in $CDCl_3$. Thus, NMR spectra must be recorded rather quickly, and the product cannot be characterized by ^{13}C NMR analysis.[47]

The [2+1] cycloaddition reaction was performed using the same conditions applied in the synthesis of the enigmol derivative. That is, 2 equivalents of NaI and 5 equivalents of $TMSCF_3$.[38] The resulting crude was directly used to perform the concomitant deprotections of the *tert*-butyloxycarbonyl (Boc) and *N,O*-isopropylidene acetal groups and *in situ* cyclopropenone formation *via* hydrolysis to obtain aminodiol **2** using a solution of trifluoroacetic acid (TFA) in water. To reverse the ammonium salt formed from the amine and to remove the excess of trifluoroacetic acid, the solution was neutralized with a solution of $NaHCO_3$ at 0 °C once the reaction was complete. Unexpectedly, upon purification by flash column chromatography the

[45] Wang, F.; Luo, T.; Hu, J.; Wang, Y.; Krishnan, H. S.; Jog, P. V.; Ganesh, S. K.; Prakash, G. K. S.; Olah, G. A. Synthesis of Gem-Difluorinated Cyclopropanes and Cyclopropenes: Trifluoromethyltrimethylsilane as a Difluorocarbene Source. *Angew. Chem.* **2011***, 123,* 7291–7295.

[46] Cheng, Z. L.; Chen, Q. Y. Difluorocarbene Chemistry: A Simple Transformation of 3,3-Gem-Difluorocyclopropenes to Cyclopropenones. *Chinese J. Chem*. **2006**, *24*, 1219–1224.

[47] Cyr, P.; Charette, A. B. Difluorocarbene Addition to Alkenes and Alkynes in Continuous Flow. *Org. Lett.* **2016**, *18*, 1988−1991.

desired product **4** was not obtained, but aminodiol **7** in an overall yield of 39%. Being compound **7** the expected deprotection result of compound **6**, it was concluded that the [2+1] cycloaddition did not occur in an acceptable yield (Scheme 5).

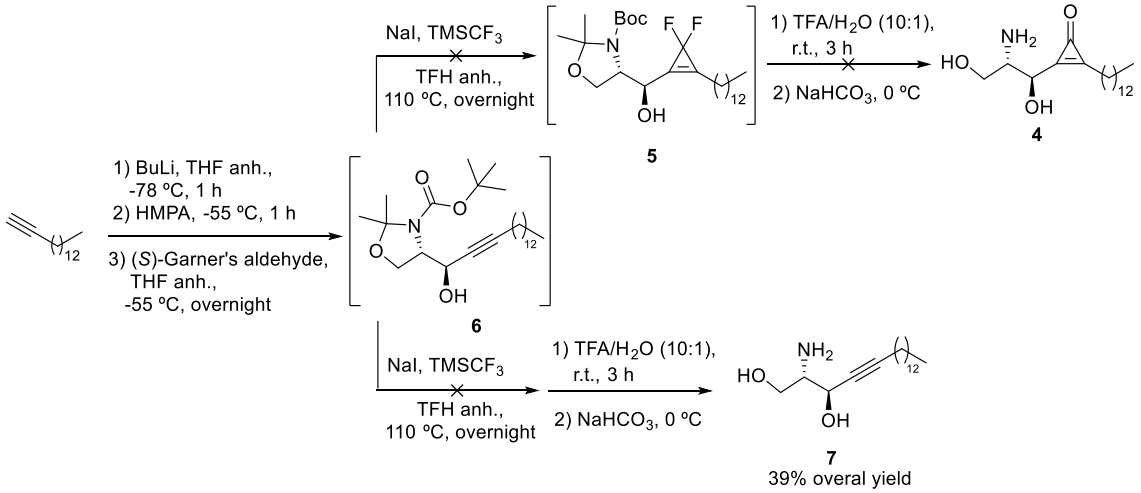

*Scheme 5: Attempted [2+1] cycloaddition reaction to obtain compound **4***

As commented before, neither product **6** nor **5** can be isolated, thus, the reactions were carried out using the crudes which greatly complicated the evaluation of which species could have affected the path of the reaction. Even so, by analysing the ^{19}F NMR spectrum done before performing the work-up of the [2+1] cycloaddition reaction it was noticed that the main product signal was a doublet located at δ -79.25 ppm with a J = 78.0 Hz, instead of the expected two doublets at around δ -100 ppm with $J_{F\text{-}F}$ = 125.0 Hz.

A tentative hypothesis that would explain the obtained result could involve the formation of a difluoromethoxy specie and subsequent hydrolysis caused by the slightly basic aqueous work-up, following the mechanism proposed by Hu *et al.* and finally delivering product **7** (Scheme 6).[48, 49, 50, 51]

[48] Xie, Q.; Ni, C.; Zhang, R.; Li, L.; Rong, J.; Hu, J. Efficient Difluoromethylation of Alcohols Using TMSCF2Br as a Unique and Practical Difluorocarbene Reagent under Mild Conditions. *Angew.Chem.Int. Ed.* **2017**, *56*, 3206–3210.

[49] Li, L.; Wang, F.; Ni, C.; Hu, J. Synthesis of *Gem* -Difluorocyclopropa(e)nes and *O*-, *S*-, *N*-, and *P*-Difluoromethylated Compounds with $TMSCF_2Br$. *Angew. Chem*. **2013**, *125*, 12616–12620.

[50] P. S. Nosik, M. O. Pashko, A. S. Poturai, D. A. Kvasha, A. E. Pashenko, A. B. Rozhenko, S. Suikov, D. M. Volochnyuk, S. V. Ryabukhin, Y. L. Yagupolskii. Monosubstituted 3,3-Difluorocyclopropenes as Bench-Table Reagents: Scope and Limitations. *Eur. J. Org. Chem*. **2021**, *2021*, 6604–6615.

[51] Cheng, Z. L.; Chen, Q. Y. Difluorocarbene Chemistry: A Simple Transformation of 3,3-Gem-Difluorocyclopropenes to Cyclopropenones. *Chinese J. Chem*. **2006**, *24*, 1219–1224.

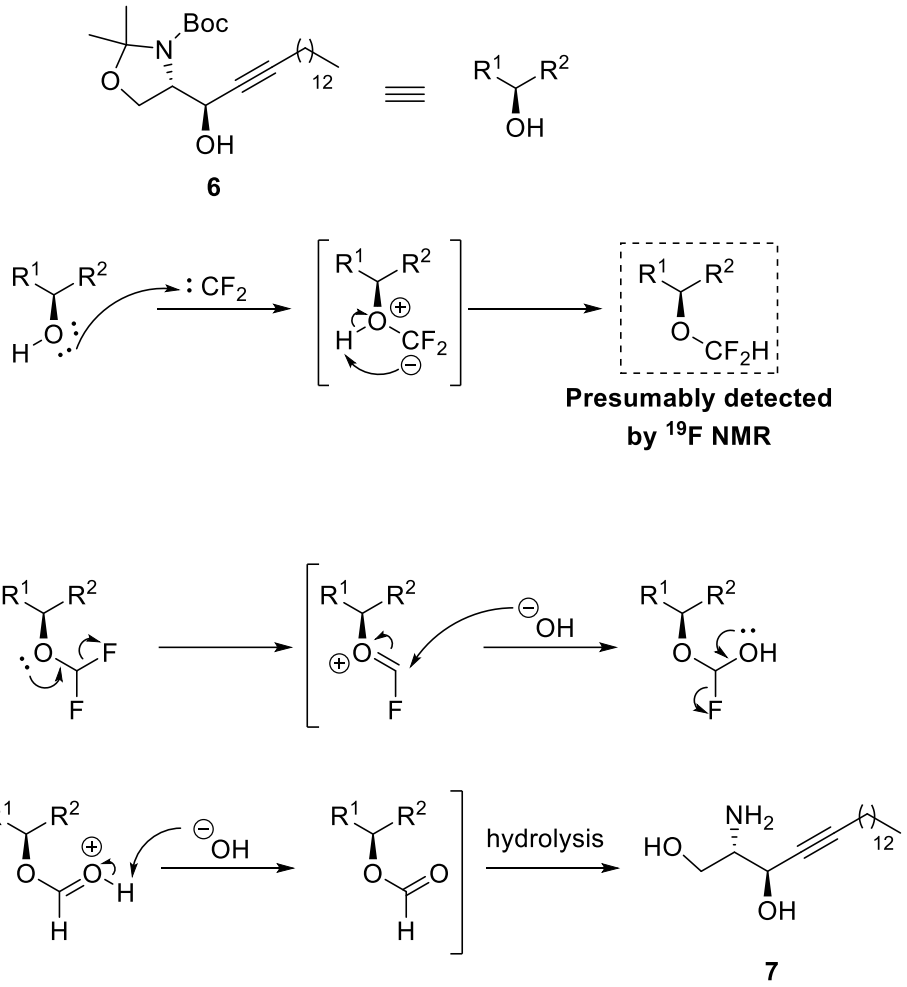

*Scheme 6: Tentative hypothesis for obtaining compound **7** based on a difluoromethoxy formation*

Bibliographic research confirmed that chemical shift, multiplicity and coupling constant were indeed compatible with the proposed difluoromethoxy specie.

The possibility of performing the *gem*-difluorocyclopropenation from product **7** was discarded, since the lone pair of electrons of the newly generated unprotected amine group would interact with the carbene, a species known for its high reactivity.[52] Besides, *gem*-difluorocyclopropenation in presence of an amine group is not only quite rarely encountered in the literature, but only for *N*-Boc dialkyl amines high yields are obtained.[53]

[52] Brahms, D. L. S.; Dailey, W. P. Fluorinated Carbenes. *Chem. Rev*. **1996**, *96*, 1585−1632.

[53] Nosik, P. S.; Gerasov, A. O.; Boiko, R. O.; Rusanov, E.; Ryabukhin, S. V; Grygorenko, O. O.; Volochnyuk, D. M. Gram-Scale Synthesis of Amines Bearing a *Gem*-Difluorocyclopropane Moiety. *Adv.Synth. Catal.* **2017**, *359*, 3126–3136.

Thus, *N*-acylation was performed before reattempting the cycloaddition reaction by using *N*-(3-Dimethylaminopropyl)-*N*'-ethyl carbodiimide (EDC) and hydroxybenzotriazole (HOBt), as coupling reagents, and octanoic acid. Product **8** was obtained in a 66% yield (Scheme 7).[54, 55]

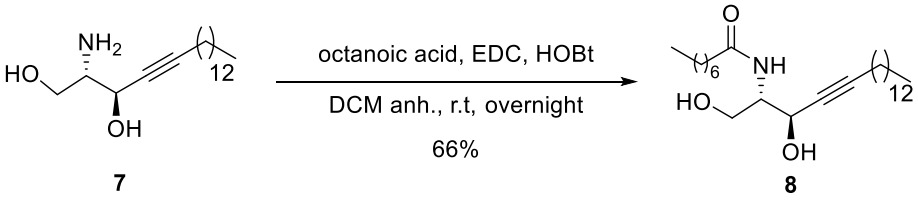

*Scheme 7: N-acylation of aminodiol **7***

The most notable ^{1}H NMR changes involve the appearance of a signal at 6.3 ppm corresponding to the proton of the newly formed amide group and the displacement of the proton geminal to the amine from 2.8 to 4.0 ppm.

With the purified amide **8** in hand, the [2+1] cycloaddition was reattempted by using the same conditions as before. The key [2+1] cycloaddition did not occur and compound **8** was recovered as the only product.

To confirm that the lack of reactivity observed was due to the substrate characteristics, the reaction was tried on a simpler substrate such as 1-pentadecyne.

As commented before, difluorocyclopropene derivatives cannot be purified *via* flash column chromatography and its ^{13}C NMR cannot be recorded due to its rapid hydrolysis towards cyclopropenone derivative. Fortunately, the crude of the reaction was clean enough to confirm the successful [2+1] cycloaddition towards difluorocyclopropene **9** unequivocally thanks to ^{19}F NMR analysis given the appearance of an apparent quadruplet as the only signal at -104.2 ppm with a coupling constant of 2.5 Hz.

Then, compound **9** reacted with silica in a mixture of Hexane/AcOH to produce cyclopropenone **10** in almost quantitative yield (Scheme 8).

[54] Valeur, E.; Bradley, M. Amide Bond Formation: Beyond the Myth of Coupling Reagents. *Chem. Soc. Rev.* **2009**, *38*, 606–631.
[55] Joullié, M. M.; Lassen, K. M. Evolution of Amide Bond Formation. *Arkivoc* **2010**, 189–250.

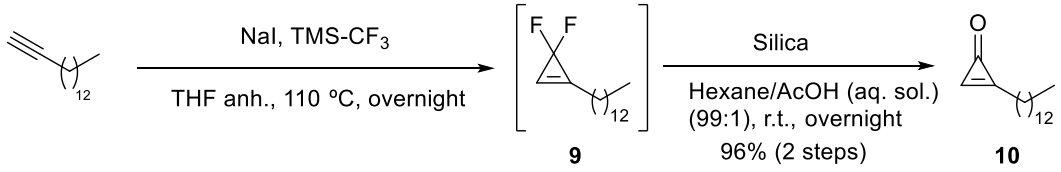

*Scheme 8: Synthesis of difluorocyclopropene **9** and subsequent transformation to cyclopropenone **10***

In view of the presented results, a new approach towards the target compound was envisioned.

3.2. Alternative approach

Since the [2+1] cycloaddition reaction was effective when performed to 1-pentadecyne, and the resulting product was a moiety of the targeted molecule, a new approach was explored based on a direct addition of a cyclopropenone derivative to the Garner's aldehyde.

In this new approach, the targeted analogue **1** would be obtained by performing an *N*-acylation over aminodiol **4**, this time containing the troublesome cyclopropenone moiety by previously generating it in a total deprotection of compound **11**. The aforementioned product should be generated from a stereoselective addition of the lithium salt of compound **12** to the (*S*)-Garner's aldehyde. Compound **12** could be obtained from the protection of the monosubstituted cyclopropenone **10**, accessible via the hydrolysis of difluorinated product **9** that was previously obtained *via* the [2+1] cycloaddition reaction (Scheme 9).

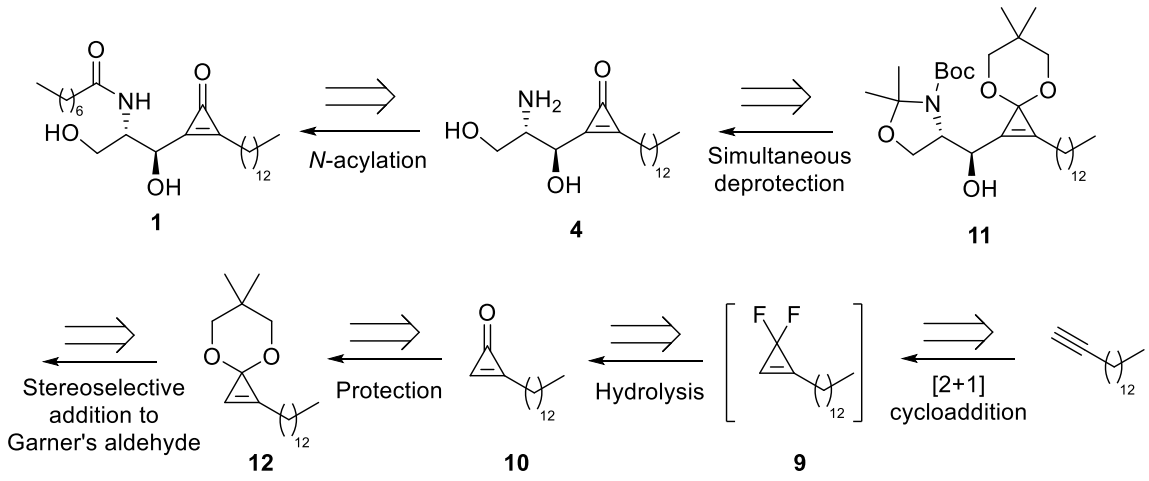

Scheme 9: Retrosynthetic analysis of the alternative approach

This new retrosynthetic pathway has some interesting traits that deemed it as a suitable alternative:

- It circumvents the troublesome [2+1] cycloaddition by effectively introducing the cyclopropenone moiety in its protected ketal form. It is important to note that its deprotection does not suppose an extra step since it can be simultaneously performed with the deprotection of the Boc and *N,O*-isopropylidene acetal groups.
- The feasibility of purification by flash column chromatography of its compounds could help in controlling the exact amount of reactants, eliminate impurities that may affect negatively the course of the reaction and, in general, to avoid some of the drawbacks of working with crudes.
- Even though there are more steps towards the final product, the rather expensive Garner's aldehyde enters in the synthesis when there are only three steps left, one less than in the previous attempt.

Direct addition of monosubstituted cyclopropenone derivatives is not possible since treatment with strong bases result in decomposition products. Thus, it was protected by converting it to its neopentilglycol ketal derivative. Notably, this is one of the few reported cyclopropenone protection methods since this moiety is usually generated *in situ* (Scheme 10).[56, 57]

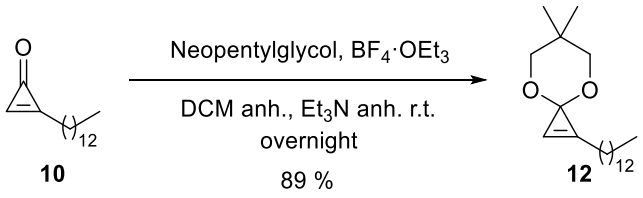

*Scheme 10: Cyclopropenone **10** protection*

Thus, the reaction of compound **10** with neopentylglycol in the presence of triethyloxonium tetrafluoroborate effectively afforded the desired product **12** in 89% yield. This transformation involves significant changes in NMR spectra, concretely the downshift in chemical shift of the proton attached to the sp^2 carbon, from 8.40 to 7.32 ppm, and the carbon originally bearing the carbonyl group, from 158.0 to 83.7 ppm.

[56] Kuzmin, A. V.; Popik, V. V. Dual Reactivity of a Photochemically-Generated Cyclic Enyne-Allene. *Chem. Commun.* **2009**, *38*, 5707–5709.
[57] Isaka, M.; Ejiri, S.; Nakamura, E. General Synthesis of Cyclopropenones and Their Acetals. *Tetrahedron* 1992, *48*, 2045–2057.

With the successful identification of compound **12**, the addition to Garner's aldehyde was performed following the same conditions applied in the initial approach, obtaining compound **11** in a 76% yield as a sole diastereomer (Scheme 11).

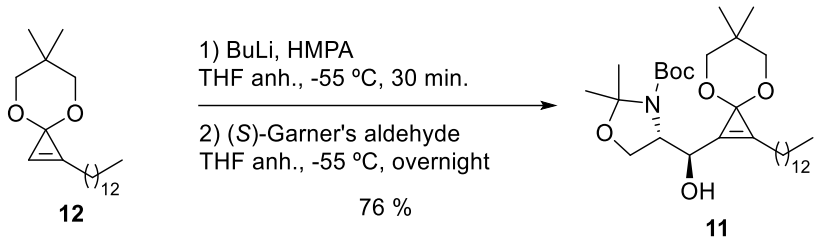

*Scheme 11: Stereoselective addition of the protected cyclopropenone derivative **12** to (S)-Garner's aldehyde*

The purification of compound **11** by flash column chromatography was rather difficult due to several compounds appearing at a similar retention factor (R_f). Given that the major offender was (*S*)-Garner's aldehyde, which had the very same R_f of the desired product, its remnants were reduced treating the reaction crude with $NaBH_4$ to form the alcohol and thus, simplify the separation. In this way, compound **11** was obtained in a 76 % yield.

^{1}H NMR analysis of product **11** cannot be done directly since most of Garner's aldehyde addition products appear as a mixture of rotamers. To overcome this situation, and to confirm this fact, ^{1}H NMR spectra were recorded at different temperatures.

As it can be seen in Figure 14, low temperatures difficult indeed the rapid interconversion between rotamers, allowing us to see them as almost singular compounds. The reverse is also true, high temperatures will cause an increase in the rate of interconversion that will permit to observe them as a sole entity with its signals being an average of the individual rotamers.

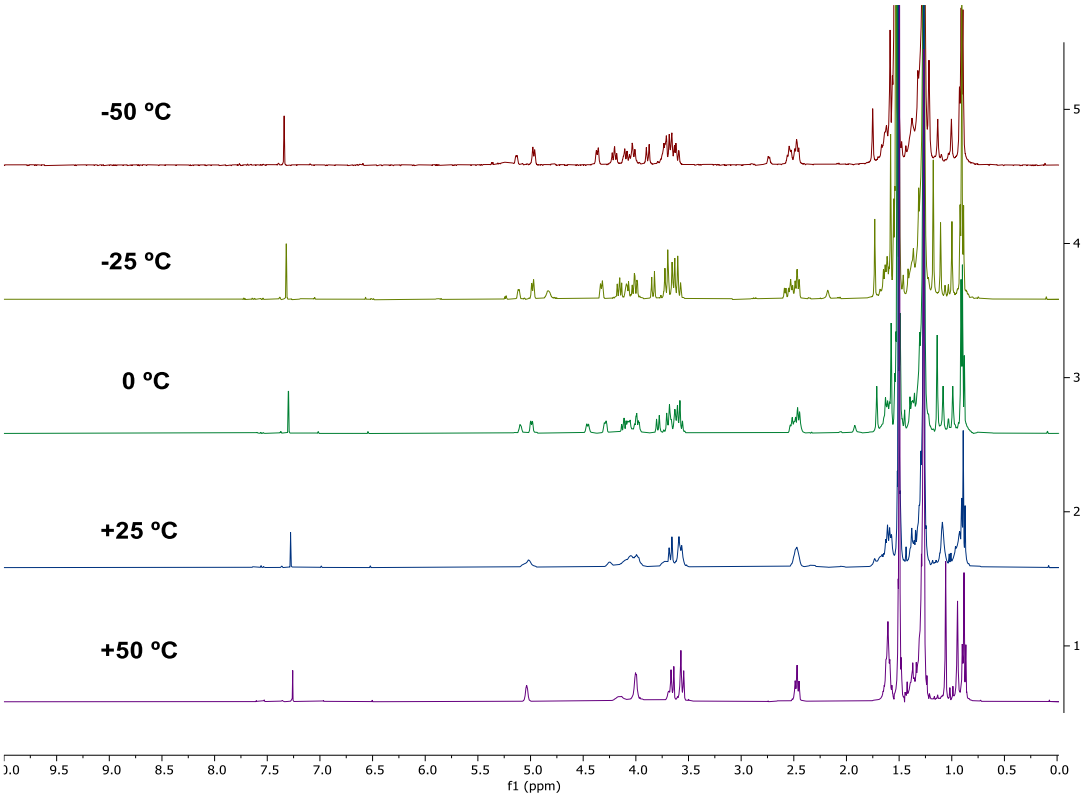

*Figure 14: ^{1}H NMR spectra of compound **11** recorded at different temperatures*

With the confirmation of the successful stereoselective addition to Garner's aldehyde, a simultaneous deprotection to generate the desired 2-amino-1,3-diol functionality and the cyclopropenone was performed using the previous conditions described. Analysis of the ^{1}H NMR spectrum of the purified product revealed that the signal corresponding to H geminal to the amine, H2, was located at 3.6 ppm instead of the expected chemical shift of 3.0 ppm. This higher chemical shift indicated that after hydrolysis, the amine had been protonated and the product was obtained as the corresponding salt (Scheme 12).

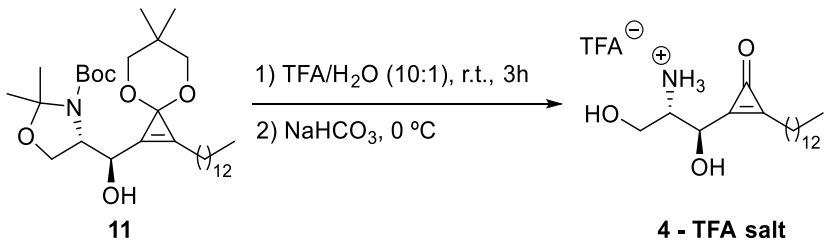

11 **4 - TFA salt**

*Scheme 12: Simultaneous deprotection of compound **11** with TFA*

Being unable to neither perform the following *N*-acylation reaction from the salt nor reverting it to product **4**, even after treating it with $NaHCO_3$ or Amberlite IRA-402, other methods of deprotection were explored.

Since the main problem was the formation of the salt due to the protonation of the amine group, a deprotection using a Lewis' acid was the initial choice. Unfortunately, the treatment of a sample of product **11** with TMSOTf resulted in its decomposition.[58] Therefore, this approach was discarded.

Suspecting that the difficulties in reverting the salt to aminodiol **4** could be caused by the TFA counterion, an acidic deprotection using another acid, HCl, was tentatively performed. To our delight, ^{1}H NMR analysis of the reaction crude revealed that the amine had been protonated, but unlike the assays performed before, product **4** could be obtained after purification by flash column chromatography with its silica being previously neutralized in a 62% yield (Scheme 13).

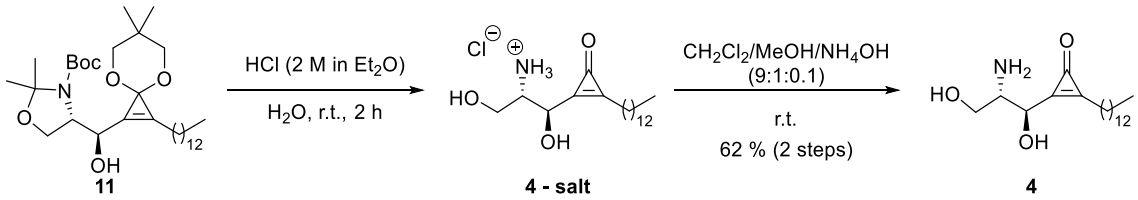

*Scheme 13: Simultaneous deprotection of compound **11** with HCl and further purification*

This was confirmed by comparing the ^{1}H NMR spectra of the reaction crude and the resulting product after purification. As can be seen in Figure 15, the reaction crude (top) features H2 at 3.6 ppm, but after the purification (bottom), the ^{1}H NMR spectrum displays H2 at a noticeably different chemical shift of 3.1 ppm, which was the expected for this compound.

[58] Potts, K. T.; Baum, J. S. Chemistry of Cyclopropenones. *Chem. Rev.* **1974,** *74*, 189–213.

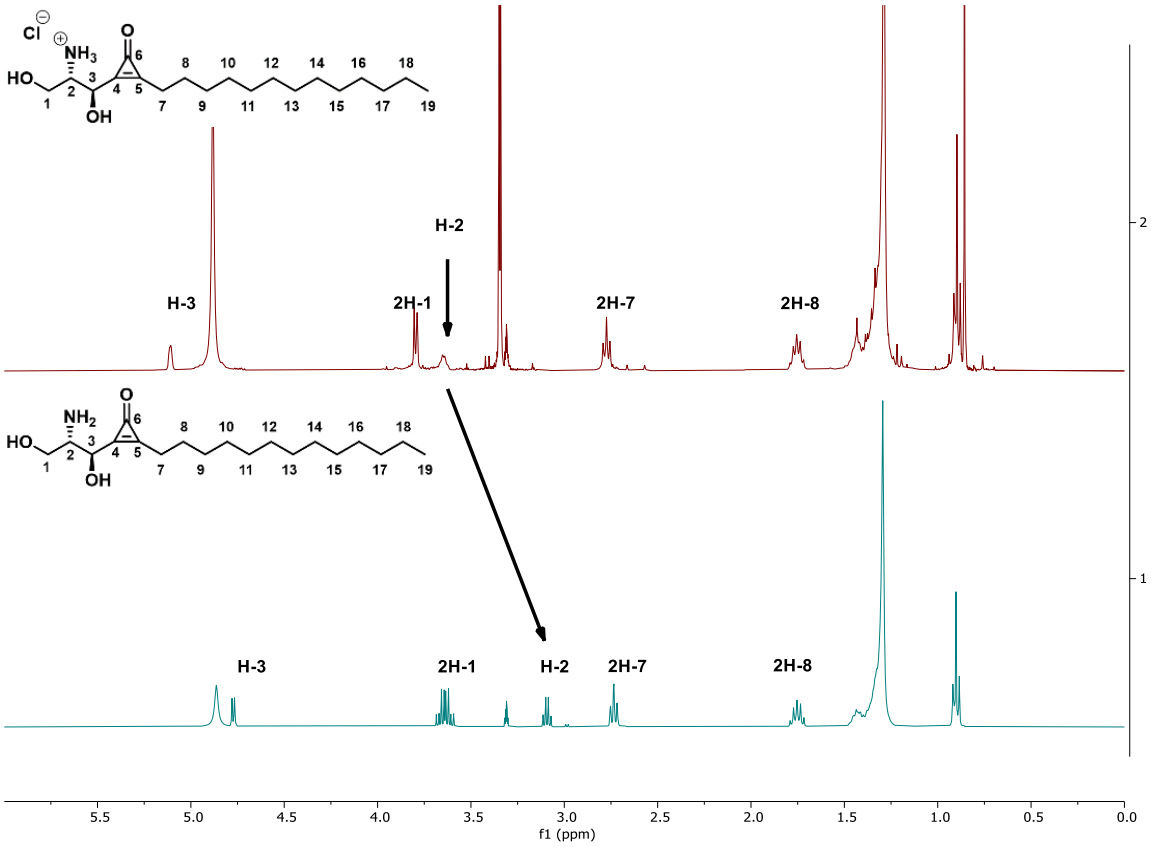

*Figure 15: ^{1}H NMR spectra comparison between the crude and the purified aminodiol **4***

With aminodiol **4** in hand only the *N*-acylation was left to obtain the desired product **1**, which was accomplished by using EDC, HOBt and octanoic acid, as done in the initial approach, obtaining compound **1** in a 60% yield (Scheme 14).

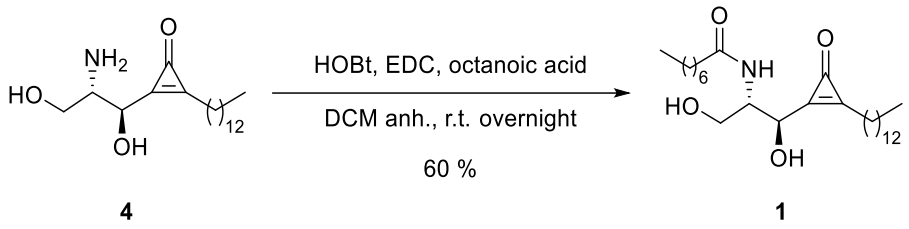

*Scheme 14: N-acylation of aminodiol **4***

Thus, the targeted ceramide analogue **1** was obtained in a 6-step synthesis in an overall yield of 24%.

The confirmation of the *anti* relative configuration, crucial for inhibitory activity, *via* X-ray crystallography (Figure 16) opened the path for a late-stage functionalization towards ceramide analogues **2** and **3**.[59]

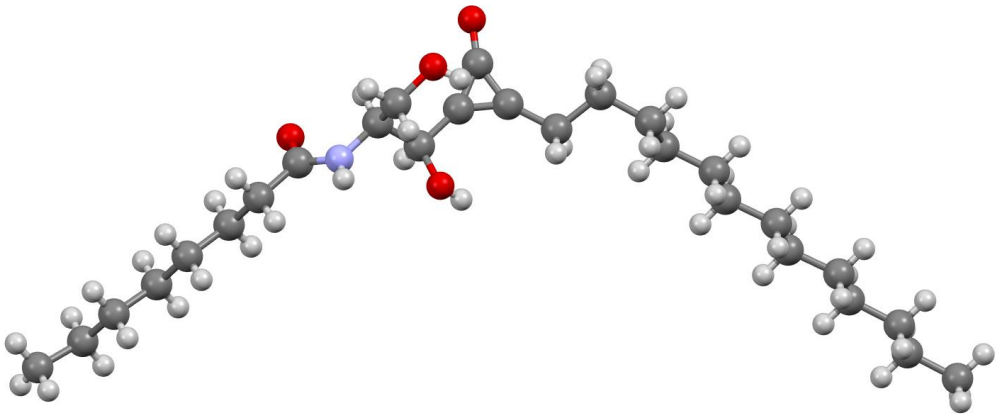

*Figure 16: X-Ray analysis of compound **1** confirmed the desired anti relative configuration*

In this sense, the singular reactivity of compound **1** was harnessed to perform a [3+2] cycloaddition following the recently published procedure by Wu *et al.* aimed at obtaining the 1,2-dichalcogen heterocyclic derivatives **2** and **3** in a late-stage functionalization.[34]

This protocol features mild reaction conditions, high efficiency, gram-scale ability, and excellent regioselectivity. Upon applying the described conditions (S power in the presence of KF and air) from compound **1** only the regioisomer **2** was detected in a 50% yield (Scheme 15).

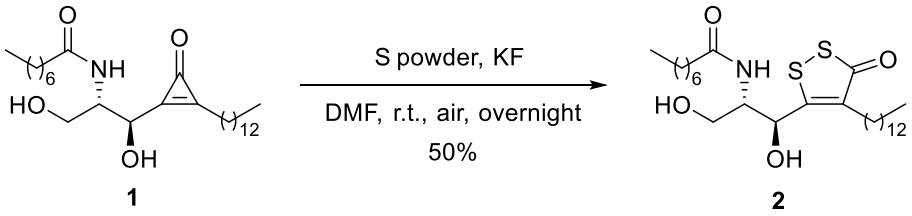

*Scheme 15: Late-stage functionalization towards compound **2***

The observed regioselectivity is in line with the few reported cases of this reaction performed on asymmetrically substituted cyclopropenones, where only one regioisomer is obtained.

^{13}C NMR analysis and, specially, HMBC are crucial to determine which regioisomer is obtained. In this sense, the chemical shift exhibited by C4 and C5, 131.3 and 167.2 ppm, respectively,

[59] Benet, J., Martínez, M. X-Ray Diffraction Unit, ICIQ.

pointed towards compound **2** given that, according to the supporting information of the cited study, the carbon in alfa to the carbonyl group is the one that experiments higher chemical deshielding. This was finally confirmed *via* HMBC analysis, since C7 was strongly coupled with the carbonyl group, while C3 was not coupled to it (Figure 17).

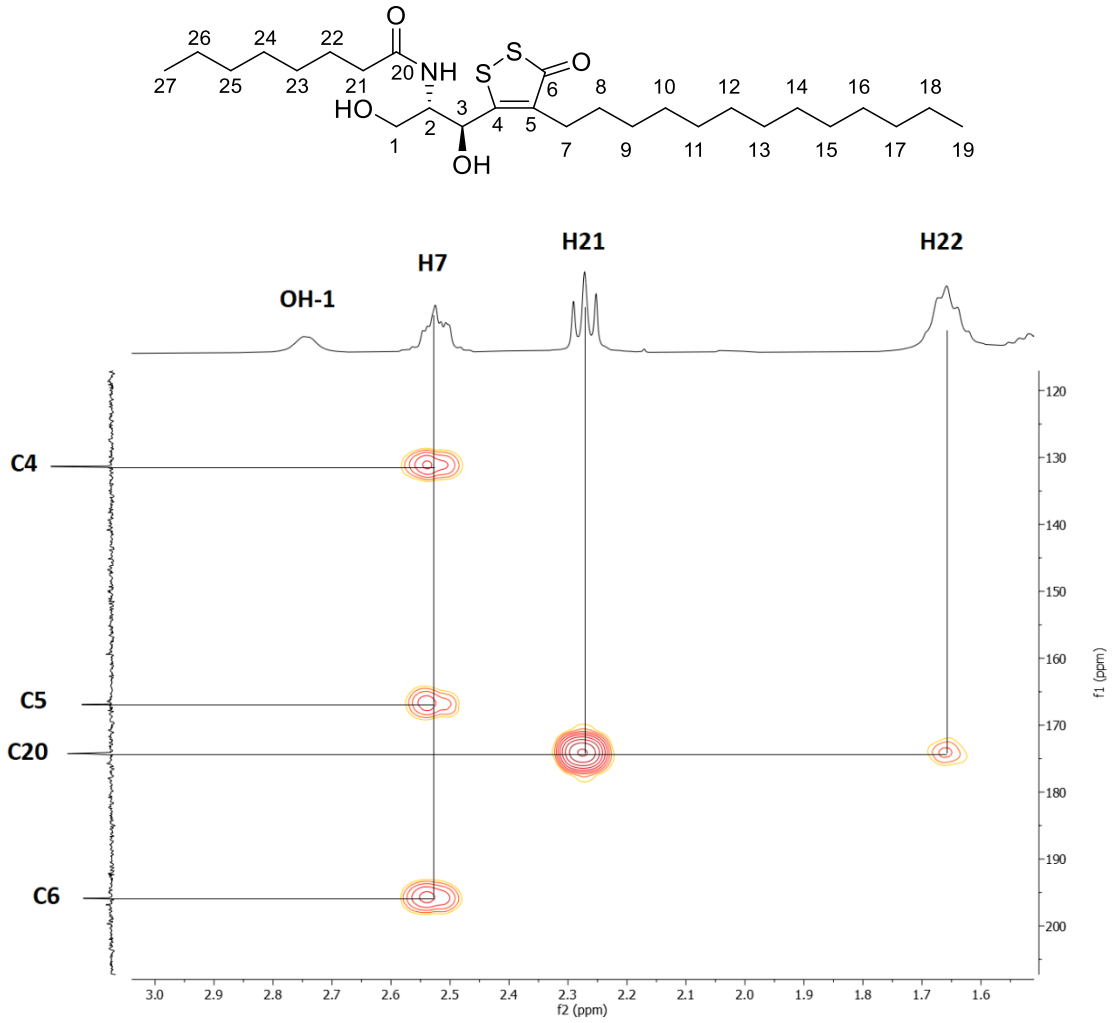

*Figure 17: HMBC analysis confirmed the obtaining of compound **2***

In the case of compound **3** and, according to the chemical shifts observed in other asymmetrically compounds bearing this moiety, it would be expected that the chemical shift of C4 and C5 were more similar, approximately at 160 and 140 ppm, respectively. Importantly, HMBC analysis would feature C3 coupled with the carbonyl group, instead of C7.

This [3+2] cycloaddition reaction involves the nucleophilic attack of S_8 to the electrophilic center of the cyclopropenone, releasing S_6 in the process. Then, the regioselectivity observed could be rationalized according to which of the two ring opening possibilities can better stabilize the

negative charge that will end up performing the cyclization by attacking the positive charged sulfur atom (Scheme 16).

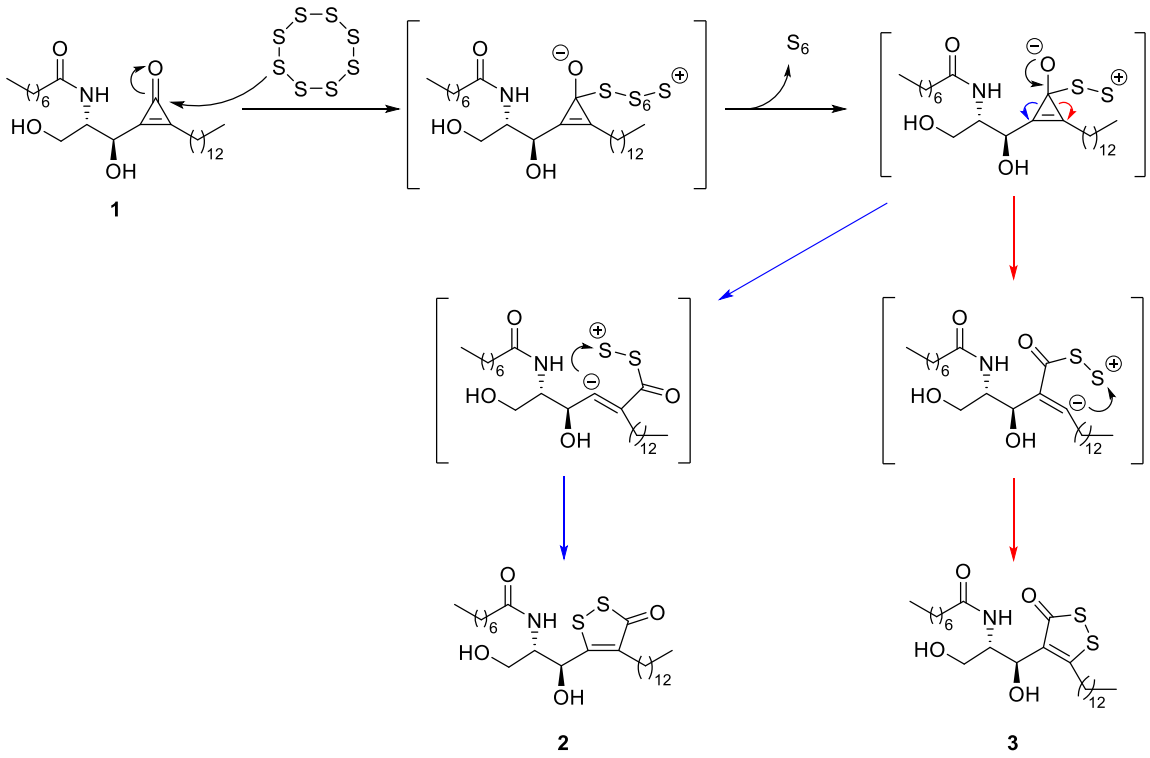

Scheme 16: Proposed mechanism for the [3+2] cycloaddition reaction

In summary, the targeted ceramide analogue **2** was obtained in an overall 7-step synthesis with 12% yield.

3.3. Biological evaluation of synthesized compounds as Des1 inhibitors

Compounds **1** and **2** have already been sent to Dra. Gemma Fabriàs laboratory (IQAC-CSIC, Barcelona) in order to evaluate their effect on Des1 activity by following the procedure reported by Llebaria *et al.*, using rat liver microsomes, employing equimolar concentrations (50 µM) of substrate (*N*-octanoylsphinganine) and each test compound. The formation of the unsaturated product will be monitored by gas chromatography coupled to mass spectrometry of the trimethylsilyl derivatives.[13] We hope to have these results in the next few days.

4. Conclusions and future work

Some conclusions have been reached with the finalization of this work:

- The initially planned synthetic pathway was based on obtaining the targeted analogues in a time-saving manner. However, the difficulties founded in the crucial [2+1] cycloaddition caused the abandonment of this pathway.
- The alternative approach is based on the combination of [2+1] difluorocyclopropenation from 1-pentadecyne, hydrolysis, and further cyclopropenone protection to form a ketal derivative that could be used in a stereoselective nucleophilic addition to (*S*)-Garner's aldehyde. X-ray crystallography confirmed its effectiveness towards obtaining the desired *anti* configuration, critical for biological activity.
- Deprotection using TFA may confine the resulting compound in its salt form. Changing the acid used, and thus the counterion, is an effective approach to avoid this problem.
- The alternative approach has been successful to obtain the targeted ceramide analogue **1** in a 6-step synthesis in an overall yield of 24%.
- A new ceramide analogue, **2**, has been synthesised with only one extra step with a late-stage functionalization that resulted completely regioselective, effectively introducing sulphur atoms to the potential Des1 inhibitor in a 7-step synthesis in an overall 12% yield.
- The inhibitory activity towards Des1 enzyme of the two synthesized targeted ceramide analogues is currently under evaluation in Prof. Gemma Fabriàs laboratory (IQAC-CSIC, Barcelona).

Future work involves the synthesis of compounds **13**, **14** and **15**, which has already been started at SINTCARB research group (Figure 18). The change towards thioketone may be beneficial regarding their inhibitory activity. Docking studies made in collaboration with Dr. Xavier Barril's research group have already confirmed their potential as Des1 inhibitors.

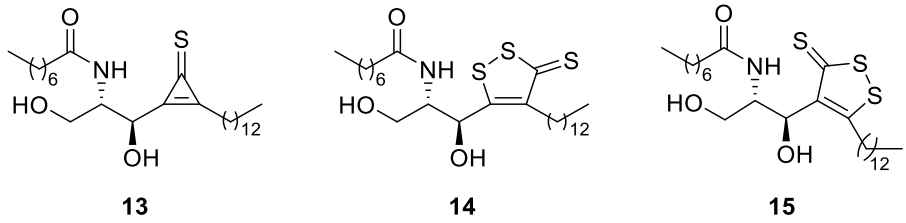

Figure 18: Future targeted analogues

Besides, if compounds **1** and **2** were effective as Des1 inhibitors it is envisioned to prepare and evaluate analogues bearing a 6 and 10 carbon *N*-acyl chain to discern how this change could affect its biological activity (Figure 19).

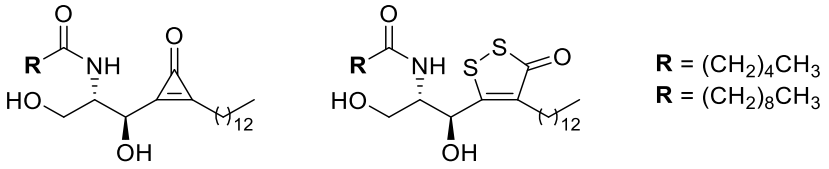

Figure 19: Envisioned N-acyl chain modifications in case the presented analogues were effective as Des1 inhibitors

5. Experimental section

5.1. General methods

All reactions sensitive to air and/or moisture were carried out in anhydrous conditions: performing vacuum-argon cycles in the flasks to be used, previously dried in the stove, as well as transferring the reagents and solvents with cannulas or syringes previously purged with argon. The procedures described below are the ones that performed with the highest yield.

IR spectra were obtained with a JASCO FT/IR-680 plus infrared spectrophotometer with Fourier transform and visualized with the SpectraManager software (JASCO®). Optical rotations (α_D^{25}) were obtained with Perkin-Elmer 241 polarimeter with a path length of 1.0 dm. Melting points (M.p.) were obtained with a Mettler Toledo DSC 822^e. High–resolution mass spectra (HRMS) were recorded on an Agilent 1100 Series LC/MSD mass spectrometer with electrospray ionization (ESI). Exact m/z values are reported in Daltons. ^{1}H, ^{13}C, ^{19}F, COSY, HSQC and HMBC NMR spectra were obtained with a Varian Mercury VX 400 and visualized with the MestreNova software (MestreLab®) in order to assign every signal.

The coupling constants (*J*) are described in Hz using the following abbreviations: s = singlet, d = doublet, t = triplet, q = quadruplet, p = quintuplet, m = multiplet, dd = doublet of doublets, dt = doublet of triplets, td = triplet of doublets, ap = apparent, br = broad. All spectra have been referenced in relation to the residual signal of the deuterated solvent used.

Thin-layer chromatography was performed on 0.25 mm E. Merck® aluminum plates coated with 60 F_{254} silica, using *p*-anisaldehyde or $KMnO_4$ as developer as indicated. Chromatographic columns were performed by passing the mentioned solvent under pressure through Fluka® or Merck® silica gel 60 (230-400 mesh).

Throughout this final master's thesis, the safety and risk prevention measures provided for current regulations have been complied. In addition, all waste generated has been disposed of under SINTCARB's standards.

5.2. Synthetic procedures and compound characterization

It must be mentioned that, for clarity, the position numeration of the compounds presented here corresponds to the normally used in sphingolipids and, therefore, it might not follow the IUPAC rules.

(2*S*,3*R*)-2-aminooctadec-4-yne-1,3-diol, 7[44]

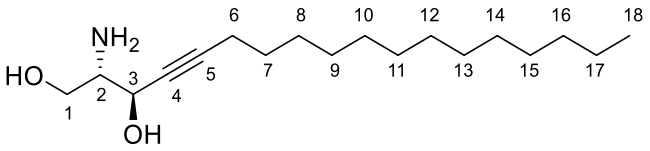

1-pentadecyne (0.30 mL, 1.14 mmol) was dissolved in dry THF (6 mL) and the solution was cooled down to -78 °C. When the temperature stabilized, BuLi (0.43 mL, 2.5 M in hexane) was added, and the temperature was raised to -55 °C. After 1 hour dry HMPA (0.27mL, 1.55 mmol) was added. After another hour (*S*)-Garner's aldehyde (207 mg, 0.90 mmol) dissolved in dry THF (1 mL) was added and the mixture was left overnight under stirring at -55 °C.

After this time NaCl (sat. sol.) was added, both phases were separated, and the aqueous phase was extracted with EtOAc. The combined organic extracts were dried over anhydrous Na_2SO_4, filtered and concentrated under vacuum to give a brownish residue.

Afterwards, NaI (340 mg, 2.26 mmol) and the previous crude were dissolved in dry THF (1 mL), and they were added to a Schlenk pression tube over argon atmosphere. $TMSCF_3$ (600 µl, 4.0 mmol) was added, the Schlenck pressure tube was sealed, and the mixture left overnight at 110 °C while vigorously stirring.

After this time $NaHCO_3$ was added, both phases were separated, and the aqueous phase was extracted with Et_2O. The combined organic extracts were dried over anhydrous Na_2SO_4 and concentrated under vacuum to give a yellowish solid residue.

A fraction composed by the previous crude (263 mg) was dissolved in a H_2O/TFA (1:10, 5.5 mL) mixture and stirred at room temperature for 1h 30 min. After this time, the reaction mixture was slowly poured into $NaHCO_3$ (sat. sol. 76 mL) solution at 0 ºC. Bubbling was observed due to neutralization of the excess of TFA.

The resulting suspension was extracted with AcOEt, the combined organic extracts were dried over anhydrous Na_2SO_4 and concentrated under vacuum to give a dark-red oily residue. The residue was purified by flash column chromatography on silica gel (DCM/MeOH/NH_4OH, 96:4:1).

Finally, product **7** was obtained as a white solid (30 mg, 39% yield).

R_f = 0.28 (DCM/MeOH/NH_4OH, 9:1:0.1); **^{1}H NMR** δ in ppm (400 MHz, CD_3OD): 4.38-4.36 (dt, $J_{3\text{-}2}$ = 5.5 Hz, $J_{3\text{-}6}$ = 2.0 Hz, 1H, H-3), 3.68 (dd, $J_{1\text{-}1'}$ = 11.0 Hz, $J_{1\text{-}2}$ = 5.5 Hz, 1H, H-1), 3.58 (dd, $J_{1'\text{-}1}$ = 11.0 Hz, $J_{1'\text{-}2}$ = 5.5 Hz, 1H, H-1'), 2.83 (q ap, J = 5.3 Hz, 1H, H-2), 2.25 (td, $J_{6\text{-}7}$ = 6.9 Hz, $J_{6\text{-}3}$ = 2.0 Hz, 2H, H-6), 1.53 (p, $J_{7\text{-}6} = J_{7\text{-}8}$ = 6.9 Hz, 2H, H-7), 1.44-1.26 (m, 20H, from H-8 to H-17), 0.90 (t, $J_{18\text{-}17}$ = 7.0

Hz, 3H, H-18); **^{13}C NMR** δ in ppm (100.6 MHz, CD_3OD): 87.8 (C-5), 79.4 (C-4), 64.7 (C-3), 63.6 (C-1), 58.7 (C-2), 33.1 (CH_2), 30.8 (CH_2), 30.8 (CH_2), 30.8 (CH_2), 30.7 (CH_2), 30.5 (CH_2), 30.3 (CH_2), 30.0 (CH_2), 29.8 (C-7), 23.8 (CH_2), 19.4 (C-6), 14.5 (C-18); **HRMS** (ESI+) for $[M+H]^+$ $C_{18}H_{36}NO_2^+$ (m/z): calculated: 298.2741, found: 298.2742.

***N*-((2*S*,3*R*)-1,3-dihydroxyoctadec-4-yn-2-yl)octanamide, 8**

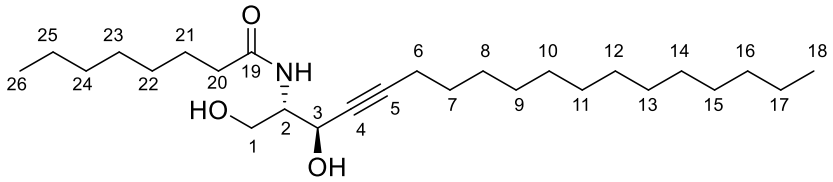

Octanoic acid (30 µL, 0.20 mmol), EDC (39 mg, 0.20 mmol) and HOBt (28.0 mg, 0.20 mmol) were dissolved in dry DCM (8.8 mL). The solution was stirred at room temperature for 45 min. The resulting mixture was added to a solution of **7** (30 mg, 0.10 mmol) dissolved in dry DCM (3.0 mL) and stirred at room temperature overnight.

After this time water was added, both phases were separated, and the aqueous phase was extracted with DCM. The combined organic extracts were dried over anhydrous Na_2SO_4, filtered and concentrated under vacuum to give a yellowish solid residue which was purified by flash column chromatography on silica gel (DCM/MeOH/NH_4OH, 96:4:1).

Finally, product **8** was obtained as a white solid (28 mg, 66% yield).

R_f = 0.36 (DCM/MeOH/NH_4OH, 95:5:2); α_D^{25} -7.2 (c 0.5, $CHCl_3$); **M.p.** 63.15 °C; **^{1}H NMR** δ in ppm (400 MHz, $CDCl_3$): 6.26 (d, J_{NH-2} = 7.7 Hz, 1H, NH), 4.61 (br s, 1H, H-3), 4.14 (dt, $J_{1-1'}$ = 11.5 Hz, J_{1-2} = 3.8 Hz, 1H, H-1), 4.07-4.02 (m, 1H, H-2), 3.79-3.74 (m, 1H, H-1'), 3.12 (d, J_{OH3-3} = 6.0 Hz, 1H, OH-3), 2.58 (dd, J_{OH1-1} = 7.4 Hz, $J_{OH1-1'}$ = 4.5 Hz, 1H, OH-1), 2.27-2.20 (m, 4H, H-6 and H-20), 1.64 (q, *J* = 6.9 Hz, 2H, H-7), 1.51 (q, *J* = 6.7 Hz, 2H, H-21), 1.31-1.26 (m, 28H, from H-8 to H-17 and from H-22 to H-25), 0.88 (t, *J* = 7.0 Hz, 6H, H-18, H-26); **^{13}C NMR** δ in ppm (100.6 MHz, $CDCl_3$): 174.3 (C-19), 88.6 (C-4), 78.0 (C-5), 65.1 (C-3), 63.0 (C-1), 54.7 (C-2), 36.9 (C-20), 32.1 (CH_2), 31.8 (CH_2), 29.8 (CH_2), 29.8 (CH_2), 29.8 (CH_2), 29.7 (CH_2), 29.5 (CH_2), 29.4 (CH_2), 29.3 (CH_2), 29.2 (CH_2), 29.1 (CH_2), 28.7 (C-21), 25.9 (C-7), 22.8 (CH_2), 22.8 (CH_2), 18.9 (C-6), 14.3 (CH_3), 14.2 (CH_3); **HRMS** (ESI+) for $[M+H]^+$ $C_{26}H_{50}NO_3^+$ (m/z): calculated: 424.3785 found: 424.3779; **IR**: 3351 (ν_{N-H}), 3280 (ν_{O-H}), 3180 (ν_{O-H}), 2955, 2914 and 2850 (ν_{CH}), 1650 ($\nu_{C=O}$), 1544 (σ_{N-H}), 1470 (σ_{O-H}), 1420 (ν_{C-N}), 1212 ($\nu_{C-O\ secondary\ alcohol}$), 1137, 1030 ($\nu_{C-O\ primary\ alcohol}$).

2-tridecylcycloprop-2-en-1-one, 10

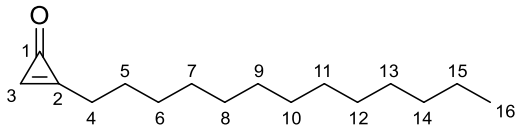

NaI (2.526 g, 16.85 mmol) and 1-pentadecyne (2 mL, 7.62 mmol) were dissolved in dry THF (10.2 mL) under argon atmosphere in a Schlenck pressure tube. Then, $TMSCF_3$ (5.63 mL, 38.09 mmol) was added, the Schlenck pressure tube was sealed, and the mixture was heated at 110 °C while vigorously stirring.

After 19 hours the reaction was stopped with the addition of $NaHCO_3$ (sat. sol.). Both phases were separated, and the aqueous phase was extracted with Et_2O. The combined organic extracts were dried over anhydrous Na_2SO_4, filtered and concentrated under vacuum to give a yellowish oily residue. The formation of the desired difluorocyclopropene was confirmed by ^{1}H and ^{19}F NMR analysis.

The obtained difluorocyclopropene was dissolved in a hexane/AcOH (99:1) mixture and treated with silica (30 g) at room temperature overnight. Afterward, the mixture was filtrated under vacuum through a filter plate with AcOEt and washed with $NaHCO_3$ (sat. sol.) The organic phase was desiccated with anhydrous Na_2SO_4 and concentrated under vacuum to give a yellowish oily residue. The residue was purified by flash column chromatography on silica gel (gradient: hexane/AcOEt, from 7:3 to 6:4).

Finally, product **10** was obtained as a white solid (1.7239 g, 96 % yield).

$\boldsymbol{R_f}$ = 0.20 (hexane/ethyl acetate, 1:1); **M.p.** = 41-42 ºC; **^{1}H NMR** (400 MHz, $CDCl_3$) δ in ppm: 8.40 (s, 1H, H-3), 2.64 (t, $J_{4\text{-}5}$ = 7.3 Hz, 2H, H-4), 1.68 (q ap, J = 7.4 Hz, 2H, H-5), 1.40-1.33 (m, 2H, H-6), 1.30-1.17 (m, 20H, from H-7 to H-15), 0.84 (t, $J_{16\text{-}15}$ = 6.6 Hz, 3H, H-16); **^{13}C NMR** (100.6 MHz, $CDCl_3$) δ in ppm: 170.3 (C-3), 158.0 (C-1), 148.2 (C-2), 32.0 (CH_2), 29.7 (CH_2), 29.7 (CH_2), 29.7 (CH_2), 29.6 (CH_2), 29.5 (CH_2), 29.4 (CH_2), 29.2 (CH_2), 29.0 (C-6), 27.5 (C-4), 25.7 (C-5), 22.7 (CH_2), 14.2 (C-16); **HRMS** (ESI+) for $[M+H]^+$ $C_{16}H_{29}O^+$ (m/z): calculated: 237.22129, found: 237.22124; **IR**: 3047 ($\nu_{C=C-H}$), 2957, 2914 and 2847 (ν_{CH}), 1804 ($\nu_{C=O}$), 1577 ($\nu_{C=C}$).

6,6-dimethyl-1-tridecyl-4,8-dioxaspiro[2.5]oct-1-ene, 12

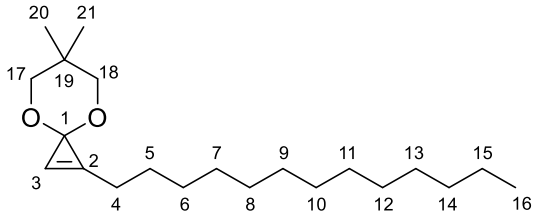

Cyclopropenone **10** (1.0053 g, 4.25 mmol) and $BF_4 \cdot OEt_3$ (1.2146 g, 6.39 mmol) were dissolved in dry DCM (7 mL) under argon atmosphere, then, the resulting mixture was vigorously stirred at room temperature for 30 min. In another flask neopentylglycol (888.4 mg, 8.53 mmol) and dry Et_3N (1.18 mL, 8.47 mmol) were dissolved under argon atmosphere in dry DCM (2.3 mL) and were added over the previous mixture dropwise over a period of 30 min. The reaction mixture was stirred overnight at room temperature.

After this time, the reaction was stopped with the addition of $NaHCO_3$ (sat. sol.). The organic phase was washed multiple times with $NaHCO_3$ (sat. sol.), and then dried with Na_2SO_4 and concentrated under vacuum to give a brown oily residue which was purified by flash column chromatography on silica gel (hexane/AcOEt, 6:4).

Finally, product **12** was obtained as a yellow liquid (1.2181 g, 89 % yield).

***R*f** = 0.30 (hexane/ethyl acetate, 9:1); **^{1}H NMR** (400 MHz, $CDCl_3$) δ in ppm: 7.32 (t, $J_{3\text{-}4}$ = 1.2 Hz, 1H, H-3), 3.63 (d, J_{gem} = 10.4 Hz, 2H, H-17 and H-18), 3.59 (d, J_{gem} = 10.4 Hz, 2H, H-17' and H-18'), 2.52 (td, $J_{4\text{-}5}$ = 7.3 Hz, $J_{4\text{-}3}$ = 1.2 Hz, 2H, H-4), 1.62 (q ap, J = 7.4 Hz, 2H, H-5), 1.40-1.25 (m, 22H, from H-6 to H-15), 1.06 (s, 3H, H-20), 1.00 (s, 3H, H-21), 0.88 (t, $J_{16\text{-}15}$ = 6.9 Hz, 3H, H-16). **^{13}C NMR** (100.6 MHz, $CDCl_3$) δ in ppm: 138.2 (C-2), 115.3 (C-3), 83.7 (C-1), 77.3 (C-17 and C-18), 32.1 (CH_2), 30.5 (C-19), 29.8 (CH_2), 29.8 (CH_2), 29.8 (CH_2), 29.8 (CH_2), 29.7 (CH_2), 29.5 (CH_2), 29.4 (CH_2), 29.3 (CH_2), 27.4 (C-5), 25.1 (C-4), 22.8 (CH_2), 22.6 (C-20 or C-21), 22.3 (C-20 or C-21), 14.3 (C-16). **HRMS** (ESI+) for $[M+H]^+$ $C_{16}H_{29}O^+$ (m/z): calculated: 323.29446 found: 323.29373. **IR**: 2952, 2924 and 2852 (ν_{CH}), 1729 ($\nu_{C=C}$), 1467 ($\nu_{\alpha\text{-}CH2}$), 1274 ($\nu_{C\text{-}O}$), 1076, 1024, 994 ($\sigma_{C=C\text{-}H}$).

***tert*-butyl (*S*)-4-((*R*)-(6,6-dimethyl-2-tridecyl-4,8-dioxaspiro[2.5]oct-1-en-1-yl)(hydroxy)methyl)-2,2-dimethyloxazolidine-3-carboxylate, 11**

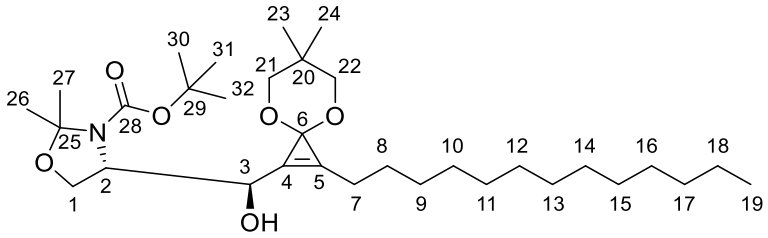

Product **12** (609.5 mg, 1.89 mmol) and HMPA (0.66 mL, 3.79 mmol) were dissolved in dry THF (8.5 mL). The solution was cooled down to -55 °C. When the temperature stabilized, BuLi (0.75 mL, 2.5 M in hexane, 1.88 mmol) was added dropwise. After 1 hour (*S*)-Garner's aldehyde (234 mg, 1.05 mmol) dissolved in dry THF (1.9 mL) was added and the mixture was left overnight under stirring at -55 °C.

After this time NH_4Cl (sat. sol.) was added, both phases were separated, and the aqueous phase was extracted with DCM. The combined organic extracts were dried over anhydrous Na_2SO_4, filtered and concentrated under vacuum to give a brownish residue which was purified by flash column chromatography on silica gel (hexane/AcOEt, 8:2).

Finally, product **11** was obtained as a colourless liquid (438 mg, 76 % yield).

R_f = 0.17 Hexane/AcOEt (8:2); α_D^{25} -8,4 (c 1.3, $CHCl_3$); **^{1}H NMR** δ in ppm (400 MHz, $CDCl_3$, 50 °C): 5.04-5.03 (m, 1H, H-3), 4.16 (br s, 1H, H-2), 4.00-3.99 (m, 2H, H-1), 3.69-3.64 (m, 2H, H-21 and H-22), 3.56 (d, J_{gem} = 11.0 Hz, 2H, H-21' and H-22'), 2.47 (t, $J_{7\text{-}8}$ = 7.5 Hz, 2H, H-7), 1.65-1.57 (m, 6H, H-26 and H-27), 1.50 (s, 9H, from H-30 to H-32), 1.37-1.26 (m, 22H, from H-8 to H-18), 1.06 (s, 3H, H-23), 0.94 (s, 3H, H-24), 0.88 (t, $J_{19\text{-}18}$ = 6.7 Hz, 3H, H-19); **^{13}C NMR** δ in ppm (100.6 MHz, $CDCl_3$): 154.0 (C-28), 130.1 (C-5), 128.7 (C-4), 95.0 (C-25), 84.9 (C-6), 81.3 (C-29), 77.7 (C-21), 77.2 (C-22), 68.5 (C-3), 64.8 (C-1), 61.4 (C-2), 32.0 (CH_2), 30.4 (C-20), 29.8 (CH_2), 29.8 (CH_2), 29.8 (CH_2), 29.8 (CH_2), 29.7 (CH_2), 29.5 (CH_2), 29.5 (CH_2), 29.4 (CH_2), 28.5 (C-30, C-31 and C-32), 27.7 (C-8), 26.2 (C-26 and C-27), 24.5 (C-7), 22.8 (CH_2), 22.6 (C-23), 22.2 (C-24), 14.3 (C-19); **HRMS** (ESI+) for $[M+H]^+$ $C_{32}H_{58}NO_6^+$ (m/z): calculated: 552.42587, found: 552.42346; **IR**: 3424 (broad, $\nu_{O\text{-}H}$), 2952, 2923 and 2850 (ν_{CH}), 1807 ($\nu_{C=O}$), 1702 ($\nu_{C=C}$), 1467 ($\sigma_{N\text{-}H}$), 1370 ($\nu_{\alpha\text{-}CH2}$), 1365 ($\sigma_{O\text{-}H}$), 1256 ($\nu_{C\text{-}O}$), 1171 ($\nu_{C\text{-}O}$), 1072 ($\nu_{C\text{-}N}$).

2-((1*R*,2*S*)-2-amino-1,3-dihydroxypropyl)-3-tridecylcycloprop-2-en-1-one, 4

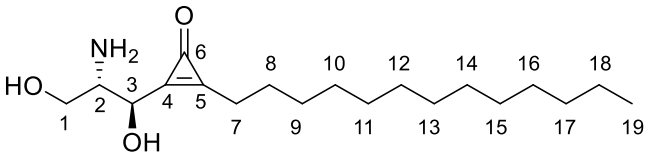

Product **11** (438 mg, 0.94 mmol) was dissolved in water (15.3 mL) and HCl (4.9 mL, 2M in Et_2O, 9.8 mmol) was added. After 3 hours under stirring at room temperature the solution was concentrated under vacuum, dried over anhydrous Na_2SO_4 and filtrated to give a brownish residue which was purified by flash column chromatography on silica gel (DCM/MeOH/NH_4OH, 95:5:1).

Finally, product **4** was obtained as a white solid (159 mg, 62% yield).

R_f = 0.20 DCM/MeOH/NH_4OH (9:1:0.1); α_D^{25} +1.6 (c 1.1, MeOH); **M.p.** = 132-133 °C; **^{1}H NMR** δ in ppm (400 MHz, CD_3OD): 4.75 (dt, J_{3-2} = 5.5 Hz, J_{3-7} = 1.0 Hz, 1H, H-3), 3.66 (dd, J_{gem} = 11.0 Hz, J_{1-2} = 5.5 Hz, 1H, H-1), 3.61 (dd, J_{gem} = 11.0 Hz, $J_{1'-2}$ = 5.5 Hz, 1H, H-1'), 3.09 (q ap, J_{2-1} = J_{2-3} = 5.5 Hz, 1H, H-2), 2.74 (td, J_{7-8} = 7.2 Hz, J_{7-3} = 1.0 Hz, 2H, H-7), 1.75 (p, J_{8-7} = J_{8-9} = 5.5 Hz, 2H, H-8), 1.46-1.26 (m, 20H, from H-9 to H-18), 0.90 (t, J_{19-18} = 7.0 Hz, 3H, H-19); **^{13}C NMR** δ in ppm (100.6 MHz, CD_3OD): 162.8 (C-6), 162.0 (C-4), 161.2 (C-5), 71.3 (C-3), 63.6 (C-1), 57.6 (C-2), 33.1 (CH_2), 30.9 (CH_2), 30.8 (CH_2), 30.8 (CH_2), 30.8 (CH_2), 30.6 (CH_2), 30.5 (CH_2), 30.4 (CH_2), 30.3 (CH_2), 27.4 (C-8), 26.8 (C-7), 23.8 (CH_2), 14.5 (C-19); **HRMS** (ESI+) for $[M+H]^+$ $C_{19}H_{36}NO_3^+$ (m/z): calculated: 326,26897, found: 326,26923; **IR**: 3284 (broad, ν_{O-H}), 2955, 2914 and 2850 (ν_{CH}), 1843 ($\nu_{C=O}$), 1617 ($\nu_{C=C}$), 1464 (σ_{N-H}), 1045 (ν_{C-O}).

***N*-((1*R*,2*S*)-1,3-dihydroxy-1-(3-oxo-2-tridecylcycloprop-1-en-1-yl)propan-2-yl)octanamide, 1**

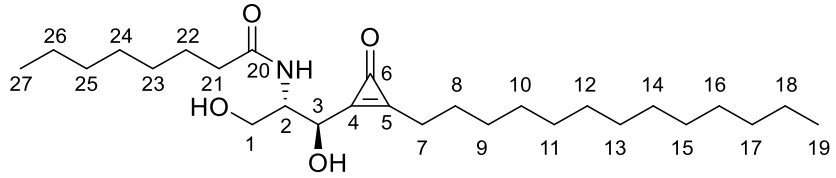

Octanoic acid (132 µL, 0.83 mmol), EDC (160 mg, 0.83 mmol) and HOBt (114 mg, 0.84 mmol) were dissolved in dry DCM (24 mL). The solution was stirred at room temperature for 45 min. The resulting mixture was added to a solution of **4** (150 mg, 0.46 mmol) dissolved in dry DCM (16 mL) and stirred at room temperature overnight.

After this time water was added, both phases were separated, and the aqueous phase was extracted with DCM. The combined organic extracts were dried over anhydrous Na_2SO_4, filtrated and concentrated under vacuum to give a yellowish solid residue which was purified by flash column chromatography on silica gel (DCM/MeOH/NH_4OH, 95:5:1). The resulting solid was trespassed to a heart-shaped flask and 3 cycles of adding pentane, waiting for a white solid to precipitate, and extracting the pentane were done.

Finally, product **1** was obtained as a white solid (126 mg, 60 % yield).

$\boldsymbol{R_f}$ = 0.09 DCM/MeOH/NH_4OH (95:5:1); $\boldsymbol{\alpha_D^{25}}$ -41.2 (c 0.5, $CHCl_3$); **M.p.** = 117-118 ºC; **^{1}H NMR** δ in ppm (400 MHz, $CDCl_3$): 6.81 (d, $J_{NH\text{-}2}$ = 5.2 Hz, 1H, NH), 5.87 (d, $J_{OH3\text{-}3}$ = 5.2 Hz, 1H, OH-3), 4.82 (d, $J_{3\text{-}OH3}$ = 5.2 Hz, 1H, H-3), 4.2 (s, 1H, H-2), 4.02-3.98 (m, 2H, OH-1 and H-1), 3.94-3.89 (m, 1H, H-1'), 2.67 (t, $J_{7\text{-}8}$ = 7.3 Hz, 2H, H-7), 2.29-2.17 (m, 2H, H-21), 1.75-1.68 (m, 2H, H-8), 1.59 (p, $J_{22\text{-}21}$ = $J_{22\text{-}23}$ = 7.3 Hz, 1H, H-22), 1.39-1.25 (m, 28H, from H-9 to H-18 and H-23 to H-26), 0.88 (t, $J_{19\text{-}18}$ = $J_{27\text{-}26}$ = 6.5 Hz, 6H, H-19 and H-27); **^{13}C NMR** δ in ppm (100.6 MHz, $CDCl_3$): 176.8 (C-20), 162.1 (C-5), 160.6 (C-4), 159.5 (C-6), 71.8 (C-3), 61.5 (C-1), 56.4 (C-2), 36.4 (C-22), 32.1 (CH_2), 31.8 (CH_2), 29.8 (CH_2), 29.8 (CH_2), 29.8 (CH_2), 29.8 (CH_2), 29.6 (CH_2), 29.5 (CH_2), 29.4 (CH_2), 29.3 (CH_2), 29.3 (CH_2), 29.1 (CH_2), 26.6 (C-8), 26.3 (C-7), 25.8 (C-22), 22.8 (CH_2), 22.8 (CH_2), 14.3 (CH_3), 14.3 (CH_3); **HRMS** (ESI+) for $[M+H]^+$ $C_{27}H_{50}NO_4^+$ (m/z): calculated: 452.37343, found: 452.37360; **IR**: 3307 (broad, $\nu_{O\text{-}H}$ and $\nu_{N\text{-}H}$), 2956, 2919 and 2852 (ν_{CH}), 1840 ($\nu_{C=O}$), 1647 ($\nu_{C=C}$), 1578 ($\nu_{C=O\ amide}$), 1548 ($\sigma_{N\text{-}H}$), 1459 ($\sigma_{O\text{-}H}$), 1073 ($\nu_{C\text{-}O}$).

***N*-((1*S*,2*S*)-1,3-dihydroxy-1-(3-oxo-4-tridecyl-3*H*-1,2-dithiol-5-yl)propan-2-yl)octanamide, 2**

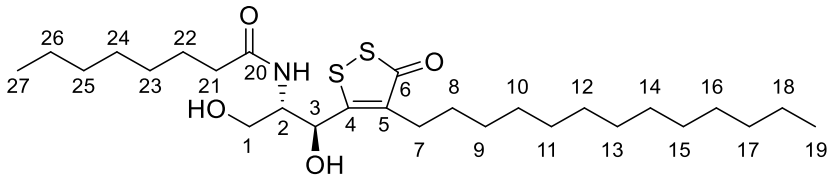

Product **1** (22 mg, 0.049 mmol), KF (5.7 mg, 0.098 mmol) and S powder (3.3 mg, 0.10 mmol) were dissolved in DMF (0.48 mL). The mixture was left under stirring overnight in air atmosphere at room temperature.

After this time NaCl (sat. sol.) was added, both phases were separated, and the aqueous phase was extracted with DCM. The combined organic extracts were washed with NaCl (sat. sol.), dried over anhydrous Na_2SO_4, filtrated and concentrated under vacuum to give a yellowish residue that was purified by flash column chromatography on silica gel (hexane/AcOEt, 6:4).

Finally, product **2** was obtained as a colourless oil (12 mg, 50% yield).

R_f = 0.18 Hexane/AcOEt (6:4); α_D^{25} 40.2 (c 1.0, $CHCl_3$); **^{1}H NMR** δ in ppm (400 MHz, $CDCl_3$): 6.51 (d, J_{NH-2} = 7.5 Hz, 1H, NH), 5.36-5.34 (m, 1H, H-3), 4.73 (br s, 1H, OH-3), 4.08-4.02 (m, 2H, H-2 and H-1), 3.71 (d, $J_{1'-1}$ = 10.5 Hz, 1H, H-1'), 2.92 (s, 1H, OH-1), 2.54-2.49 (m, 2H, H-7) 2.27 (t, J_{21-22} = 7.4 Hz, 2H, H-21), 1.65 (p, J_{22-21} = J_{22-23} = 7.4 Hz, 1H, H-22), 1.55-1.46 (m, 2H, H-8), 1.35-1.26 (m, 28H, from H-9 to H-18 and H-23 to H-26), 0.90-0.85 (m, 6H, H-19 and H-27); **^{13}C NMR** δ in ppm (100.6 MHz, $CDCl_3$): 196.0 (C-6), 174.3 (C-20), 167.2 (C-5), 131.3 (C-4), 73.8 (C-3), 61.6 (C-1), 53.7 (C-2), 36.8 (C-21), 32.1 (CH_2), 31.8 (CH_2), 29.9 (CH_2), 29.8 (CH_2), 29.8 (CH_2), 29.8 (CH_2), 29.7 (CH_2), 29.7 (CH_2), 29.6 (CH_2), 29.5 (CH_2), 29.4 (CH_2), 29.1 (CH_2), 28.4 (C-8), 27.9 (C-7), 25.8 (C-22), 22.8 (CH_2), 22.8 (CH_2), 14.3 (CH_3), 14.2 (CH_3); **HRMS** (ESI-) for $[M+Cl]^-$ $C_{27}H_{50}NO_4S_2Cl^-$ (m/z): calculated: 550.27970, found: 550.27991; **IR**: 3325 (broad, ν_{O-H} and ν_{N-H}), 2955, 2920 and 2853 (ν_{CH}), 1644 ($\nu_{C=O}$), 1626 ($\nu_{C=O\ amide}$), 1562 (σ_{N-H}), 1544, 1461 (σ_{O-H}), 1376 ($\nu_{\alpha-CH2}$), 1262 ($\nu_{C-O\ secondary\ alcohol}$), 1121 ($\nu_{C-N}$), 1075 ($\nu_{C-O\ primary\ alcohol}$), 600 ($\nu_{S-S}$).